Progress in Additive Manufacturing (2025) 10:4305–4325
https://doi.org/10.1007/s40964-024-00856-x

REVIEW ARTICLE

Recent advances in the AlSi10Mg materials fabrication by selective laser melting: process parameters, optimization, low-velocity and ballistic impact responses

Faik Yilan[1] · **Recep Ekici**[2] · **Levent Urtekin**[1]

Received: 12 August 2024 / Accepted: 28 October 2024 / Published online: 15 November 2024

Abstract

The global landscape underscores the critical need for nations to develop indigenous production capabilities to fulfill both their defense requirements and those of allied nations. This necessity is increasingly addressed not through mere augmentation of investments in armor and ballistic-resistant structures, but by executing integrative projects and establishing robust R&D infrastructures. In this context, Selective Laser Melting (SLM) technology, a subset of additive manufacturing, presents a significant opportunity due to its proficiency in fabricating intricate geometries. This review meticulously examines the impact of variable process parameters on the mechanical properties of SLM-fabricated AlSi10Mg components. Utilizing Response Surface Methodology (RSM), the study systematically analyzes data derived from literature to identify the most optimal parameters. Furthermore, the review encompasses recent investigations into the low-speed impact and ballistic performance of SLM AlSi10Mg alloys, providing a comprehensive understanding of their applicability in defense-related applications. Key areas of focus include the influence of laser power, scanning speed, hatch spacing, and layer thickness on the resultant mechanical properties, such as density, tensile strength, and fatigue resistance. The review also delves into the post-processing techniques that enhance the performance of SLM parts, including heat treatment and surface finishing. By integrating findings from various studies, this review article aims to elucidate the potential of SLM technology in advancing the production of high-performance materials for defense applications, thereby contributing to the strategic autonomy of nations in the defense sector.

✉ Faik Yilan
faik.yilan@ahievran.edu.tr

Recep Ekici
rekici@erciyes.edu.tr

Levent Urtekin
levent.urtekin@ahievran.edu.tr

[1] Department of Mechanical Engineering, Kırşehir Ahi Evran University, Kırşehir, Turkey

[2] Department of Mechanical Engineering, Erciyes University, Kayseri, Turkey

Graphical abstract

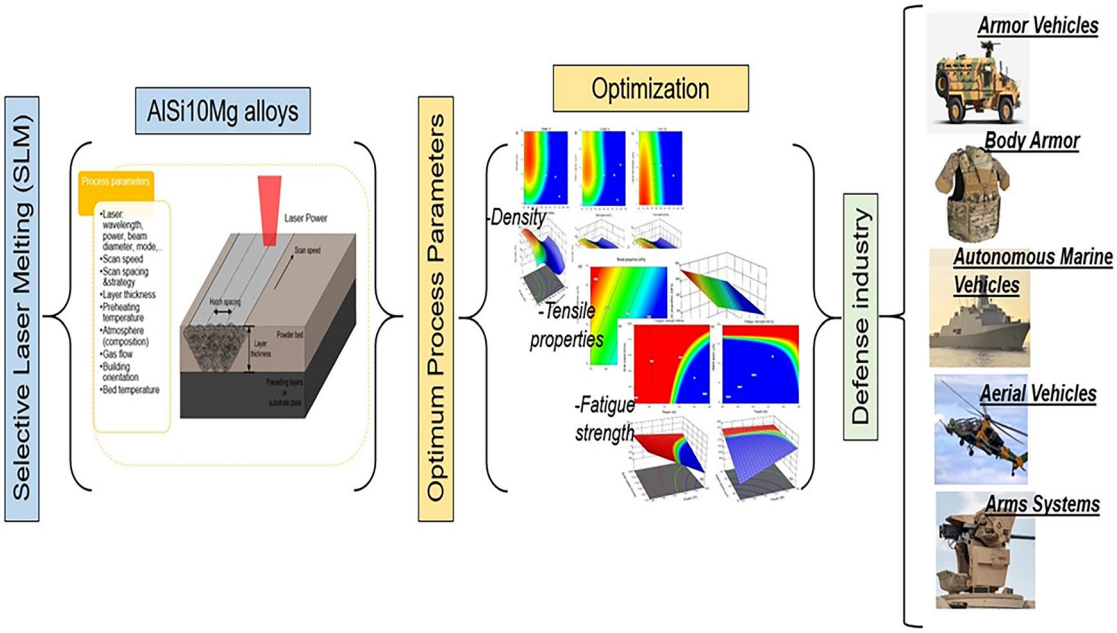

Keywords Selective laser melting · AlSi10Mg · Process parameters · ANOVA · Ballistic

1 Introduction

In today's world, many developing countries are making significant strides in the defense industry. Due to insufficient technological infrastructure, these countries often rely on importing weapons and armored vehicles, which increases defense budgets and foreign dependency. Therefore, a priority for developing countries is to increase the production of armored vehicles and new materials from domestic resources to avoid economic and environmental issues. This interconnected problem affects various sectors in a cyclical pattern due to cause–effect relationships. A current example is the Russian–Ukrainian war, which poses a threat to individuals, society, and multiple sectors, including the defense industry, due to its economic and purchasing impacts on global market stakeholders. Consequently, countries aim to control defense budgets and reduce foreign dependency. It is imperative to create innovative policies supporting scientific studies and technological advancements in ballistic and armor systems. The defense industry is a priority development area in Turkey's Development Plans by the Strategy and Budget Presidency of the Republic of Turkey.

Improving the performance of materials used in armored vehicles is a crucial goal for the defense industry. High-strength steels, ceramics, composites, and multi-materials are commonly used armor materials. R&D and investment activities continue to focus on producing lightweight, high-strength products domestically for sectors like the defense industry. These new materials will enable armored vehicles to move faster and provide more effective defense performance (Fig. 1).

Aluminum alloys are one of the most commonly used armor materials in armored vehicles due to their low density, corrosion resistance, superior weldability and high specific strength. Therefore, aluminum alloys offer a cost-effective solution for low-cost armor production due to their outstanding mechanical strength and ballistic properties [1–4]. However, AlSi10Mg alloy is one of the easiest alloys to be produced by selective laser melting among aluminum alloys, thanks to its metallurgical characteristics [5, 6]. Hence, AlSi10Mg alloy is widely used in industries, such as automotive, aerospace, etc. [7]. For the mentioned reasons, AlSi10Mg alloys were examined in most of the studies on selective laser melting, which is the powder bed fusion technique of additive manufacturing between 2010 and 2024 [8–11]. As can be seen from these studies, AlSi10Mg alloys stand out as an effective method in terms of selective laser melting technology, which is a promising object production method [12, 13]. These articles have been researched in many countries. When we look at the distribution of studies by country in Fig. 2, it is observed that the majority of

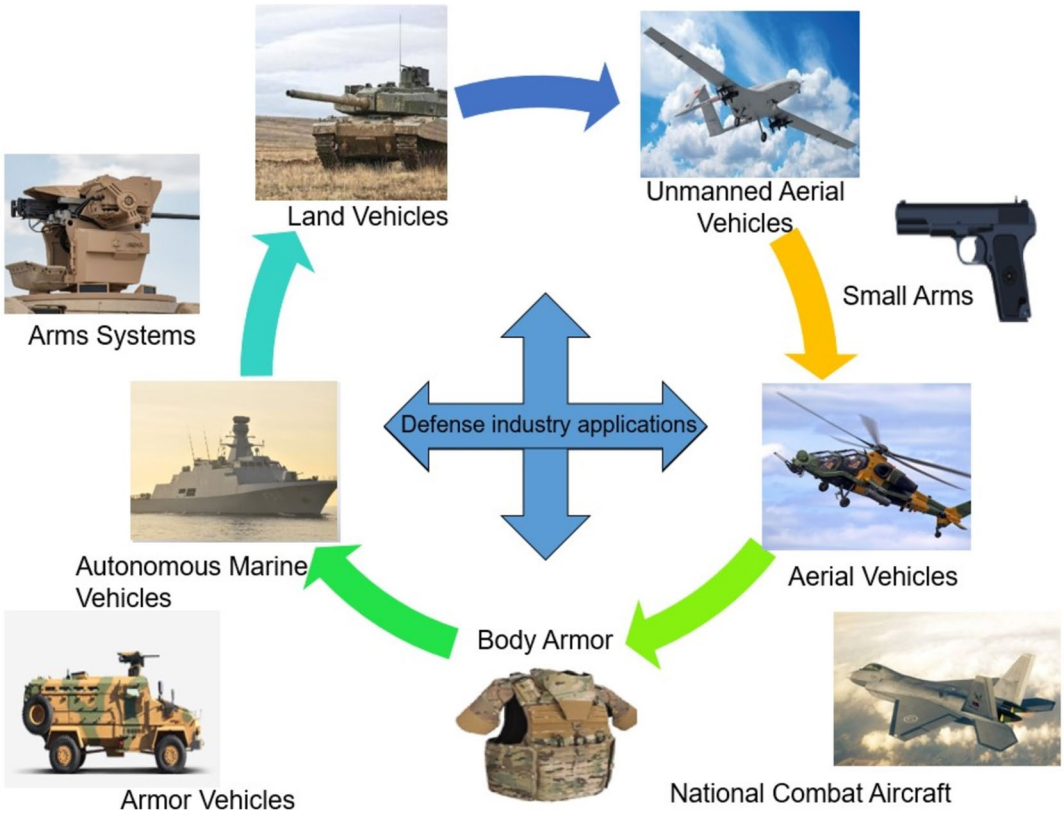

Fig. 1 Activity areas of defense technology

the studies are in the USA and China. It is thought that the main reason for this is due to the high number of researchers and the amount of support given by the US and Chinese governments to scientific studies. Moreover, the institutions that standardize the experimental methods used in the performance evaluation of the selective laser melting technique are generally located in the USA. Under the leadership of these institutions, it is thought that most of the obstacles facing researchers in the USA do not exist [14]. Researchers in Turkey face cost challenges in their studies related to master's and doctoral theses, which naturally causes them to lag behind other countries. This study systematically evaluates the results of optimized production parameters/strategies using the Analysis of Variance (ANOVA) method. The goal is to adopt time, cost, and material savings in various sector applications, especially in defense and aerospace, by selecting a fewer number of optimal production parameters/methods. The results obtained from this compilation study are expected to provide significant information to the literature and serve as a valuable reference for researchers and designers in this field.

This literature study examines the sustainable, reliable and highly effective defense approaches of AlSi10Mg armor materials used in defense industry equipment to be produced from selective laser melting process parameters/strategies. In this context, comprehensive examinations and evaluations of AlSi10Mg parts in the literature are carried out in terms of process variability, especially their mechanical performance, and optimum quality [15, 16]. Most of the researchers have thoroughly investigated the understanding of parametric studies [17, 18], defects and remedies [19–21], metallurgical [22–24] and mechanical performances [25–28] of AlSi10Mg alloys produced by SLM. In particular, numerous studies have been conducted to optimize SLM processing parameters to obtain high-density aluminum components [29]. These features include laser power, scanning range, scanning speed, scanning strategy, and build direction, which are primarily examined as adjustable variables. It is argued that achieving appropriate energy levels is crucial in the manufacturing process of fully dense components. Excessive or insufficient laser input energy may cause energy to be transferred to the material and cause errors to occur in the desired parts. Zhichao Dong et al. [30] investigated the importance of process parameters on the microstructure of AlSi10Mg alloy produced by SLM was determined. The AlSi10Mg alloy, due to its low viscosity and high thermal conductivity, results in poor laser absorption, necessitating increased laser power. Therefore, ensuring a high laser

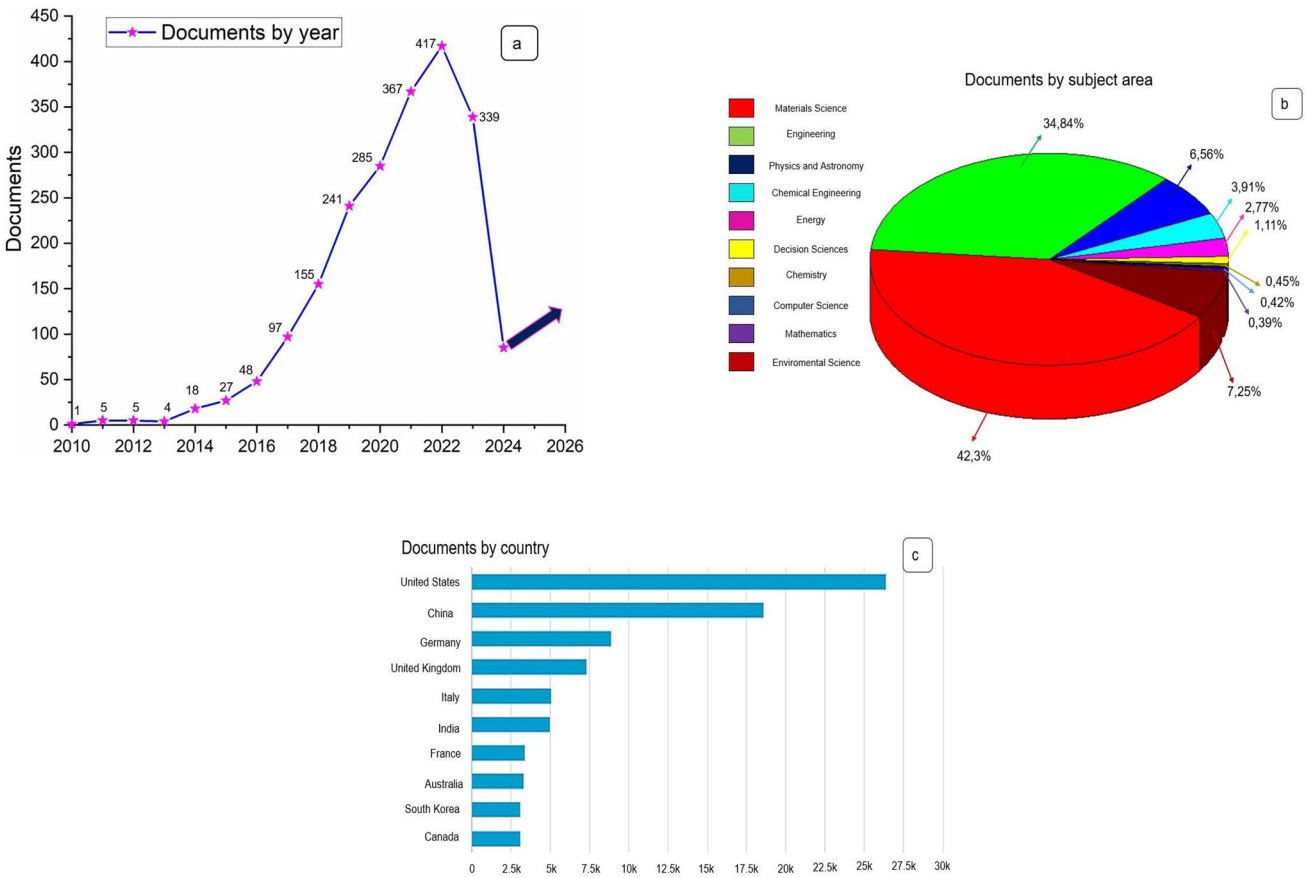

Fig. 2 In documents reported in the Elsevier on SLM and AlSi10Mg alloys **a** by year **b** by subject area and **c** by country

power constant and a thin microstructure in SLM production is crucial for maintaining good mechanical properties. This alloy's low viscosity and high thermal conductivity necessitate more power. Awd et al. [31] studied the mechanical and microstructure properties of AlSi10Mg alloys using the SLM method using three scanning angles. They found that a 90°-scanning angle resulted in 7 times higher pore density, 8% higher strength, and 30% lower fracture stress, indicating a direct impact of scanning angle. Majeed et al. [32] studied the impact of laser power, scanning speed, overlap ratio, and scanning distance on surface quality in the SLM method. They found an increase in surface roughness with increasing laser power, with a negative correlation with overlap ratio and scanning speed. The optimal process parameters were 0.32 kW laser power, 0.6 m/s scanning speed, 35% overlap rate, and 88.7 mm scanning distance. Li et al. [33] produced 7 pieces of AlSi10Mg alloy using different angles using the SLM method. The highest hardness was 154.44 HV at 45°, while the best tensile strength was 463.54 MPa at 60°, with 283.37 MPa yield strength and 9.25% elongation. The exact influence of process design parameters on physical and mechanical behavior and hence the suitability of AlSi10Mg parts produced via SLM are still not fully understood. Therefore, determining the mechanical behavior of SLM parts as well as the influence of process design parameters is vital to predict their performance in service.

Response surface methodology (DoE), also referred to as the Taguchi method, is a statistical technique for developing an experimental design with the goal of optimizing process responses (e.g., toward a maximum and minimum) and determining an approximation model between input and output parameters [34, 35]. It is a compilation of mathematical and statistical information that is helpful for modeling and problem-solving in engineering. This technique's primary goal is to optimize the response surface as it is impacted by different process parameters. Consequently, the Taguchi approach can be regarded as an effective design technique that maximizes process performance while requiring the fewest number of experiments. It lowers expenses associated with experimental research and streamlines the production and testing processes, and estimates performance variables by converting test results into S/N ratios [36–38]. This makes the variations between the test samples clear. There are almost a few studies investigating the mechanical behavior of process parameters used in SLM on AlSi10Mg alloys using the Taguchi approach, including the following:

- Read et al. [12] investigated the effect of process parameters in the SLM technique on porosity formation in AlSi10Mg alloy. Using a statistical experimental design, they established a correlation between this design and the energy density model. The findings showed that laser power, scan speed, and the interaction between scan speed and scan range significantly impact porosity formation. Optimum process parameters were determined by applying a statistical approach aimed at minimizing the porosity ratio.
- Liu et al. [39] used the Taguchi approach to optimize the processing parameters and obtain a completely dense AlSi10Mg sample.

As can be clearly seen in the literature, separate changes in the mechanical properties were examined along with the changes in the values of the 4 relevant parameters. However, according to the authors' current knowledge, there is no study to determine the most effective design parameters by evaluating all features together from a more comprehensive perspective. In addition, all evaluations in the literature have been made on how mechanical properties are affected by changing the values of only a single process parameter. However, it is thought that all process parameters change together and how this is reflected in the results is very important in terms of optimization. In this context, we think that there is a serious gap in the literature to determine the most effective process parameters with main and interaction effects. In order to close this gap, a statistical model was developed using data from studies previously introduced in the literature. This established model was tested with ANOVA results. All evaluations were made based on this model. The main general innovations in this work are:

- To introduce in full detail, SLM technology has a promising potential that will help reduce production costs and increase production efficiency in order to meet the demands in the defense industry,
- To summarize the results of density, tensile properties and fatigue strength of AlSi10Mg alloy materials are produced from different parameters in the SLM process in a single table. In this way, it will enable the determination of the most effective parameter and give ideas about whether there are interactions between the parameters with ANOVA analysis,
- Optimizing the SLM process design parameters of AlSi10Mg alloy materials for impact protection is still an issue to be solved. As far as the authors know from scientific studies, there is no study yet on the optimum process parameters on the ballistic and low-speed impact behavior of the AlSi10Mg alloy produced with the additive manufacturing-based SLM technique. For this reason, to ensure the effects of the potential comprehensive ballistics, literature studies carried out so far are easily noticed.

2 Selective laser melting (SLM)

Selective laser melting (SLM) is a direct AM technology with a controlled melting of metal powder, which is used to produce almost completely dense parts with high complexity [40, 41]. The SLM production process comprises several stages, starting with the compilation of CAD data and concluding with the removal of the finished goods from the construction platform [42]. In the process of manufacturing design items, stereolithography (STL) files are generated using specific software. These files are used to produce support structures and load CAD data into the SLM device. Additionally, the software is used to slice the model into layers (Slics) and establish the path for laser scanning. The production process commences with the deposition of a fine layer of metal particles onto the platform within the construction zone [43]. Following the application of the powder, a laser with high energy density is employed to heat and merge specific regions based on processed data. Upon completion of the laser scan, the building platform descends, a layer of powder is deposited on it, and the laser proceeds to scan a fresh layer. This procedure is repeated for consecutive layers of powder until the final model product is fully constructed (video accessed February 2, 2024, at 3D Printing Technologies: Selective Laser Melting (SLM) (https://www.youtube.com) [44, 45].

The main advantages of the SLM method		References
Design flexibility	• When designing, instead of creating a large number of simple parts, a smaller amount of design products can be obtained, thus speeding up reverse engineering work • The lightness, material savings and esthetic appearance of the materials produced meet the expectations in terms of engineering	[46–48]
Cost of geometric complexity	• This method facilitates the production of complex geometries in the desired form, and as the sample to be produced geometrically becomes smaller, production becomes easier • It was a method that added privilege in the increasingly accelerating product development and rapid production of different designs	[49]

The main advantages of the SLM method		References
Dimensional accuracy	• It is possible to produce parts with a complex lattice structure with high accuracy and a very small margin of error • Products produced with this method enable a wide variety of products in the fields of medicine, automotive, aerospace and defense industries and provide services in these fields	[50, 51]
Need for assemblage	• It directly enables the production of parts, which allows you to avoid some costs such as maintenance expenses, the use of assembly elements, and extra labor • In complex geometries that are desired to be produced, producing this part as a whole, instead of assembling it with more than one piece inside, makes that part more efficient in heat transfer and energy applications	[52]
Time and cost efficiency in production run	• Thanks to its practicality, this method enables the creation of a highly functional, lightweight product with mechanical properties suitable for the design, with maximum design geometry • It can be used in the production of systems, mechanisms or elements designed in engineering and R&D activities	[53, 54]

The fiber lasers are used in SLM systems and they work with a continuous laser pulse where the laser has almost no fluctuation over time. The laser beam coming out of the laser source is directed by galvano mirrors and interacts with the planned scanning speed on the production platform where the powder is laid. In the SLM system, the heat input provided by the laser radiation is absorbed by the powder, and unlike the selective laser sintering method, complete melting is achieved and a bond with the previous layer is ensured. After the part of the work piece is created, the part is produced by combining it with the previous layer and continuing this repetition until the whole part is created (see Fig. 3). Surface roughness is in the range of 5–15 µm (µm) and layer thickness is in the range of 10–100 µm. In the SLM production method, metal materials, such as cobalt-chrome, stainless steel, aluminum and titanium alloys, can be produced. A fiber laser with a power of 100–400 Watt (W) is used during

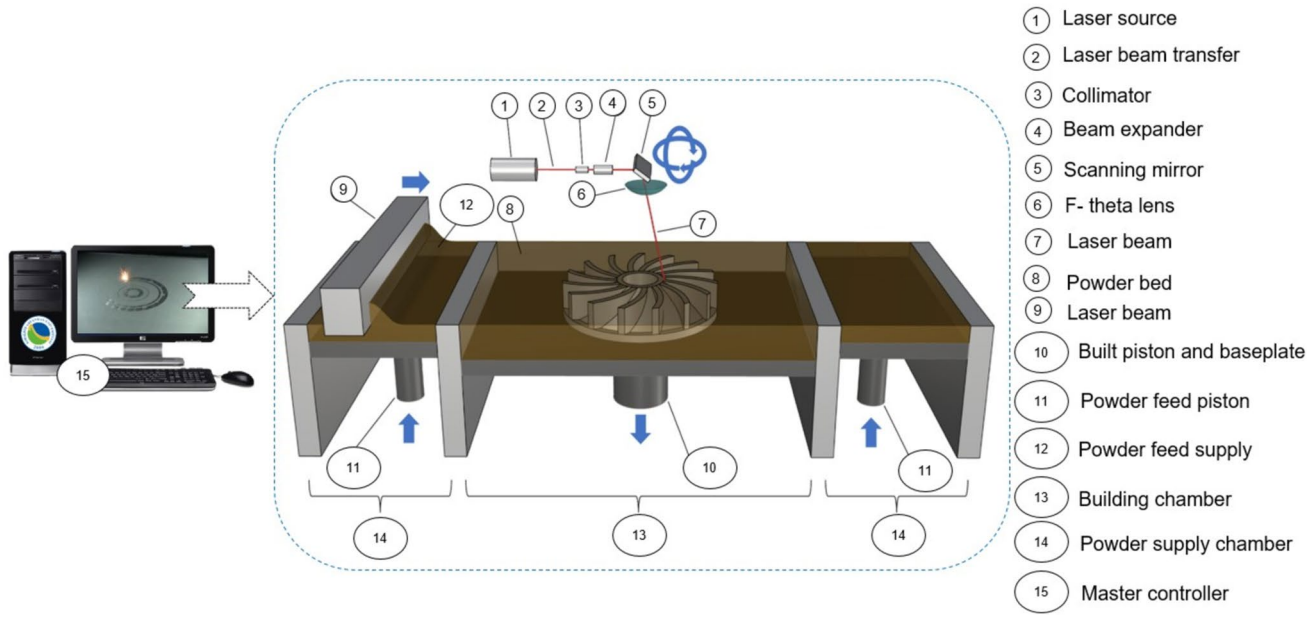

Fig. 3 Operation scheme of SLM technologies [59]

the melting process [55, 56]. With the help of laser beam, the molten parts become solid in that layer and the production platform is lowered to create the next layer. After the layer is lowered, the powder laying process and melting process with the help of laser beam are repeated and these processes are repeated until the desired geometry is obtained. Processes are carried out under different protective gas atmospheres depending on the metal materials used. As an example of these environments, if production is made from stainless steel powder, nitrogen gas is used as a protective gas. If aluminum and its alloy powders are used, argon gas is used as a protective gas. There are two main reasons why production is carried out with protective gas. The first is that it causes oxidation depending on the metallic material used during production or because the temperature is too high as an operating parameter. The second reason is that the laser beam is not deflected in the environment during production [57, 58].

2.1 SLM process parameters

In the SLM method, production is affected by more than one variable. It is possible to examine these variables in two groups. First, the parameters related to the laser beam, and second, the scanning paths and the desired geometry. Parameters related to laser; speed of the laser, diameter at which the laser focuses, power of the laser. parameters related to another variable, geometry, are; parameters, such as the direction to be built, scanning distance, desired layer thickness [60–63]. Figure 4 outlines the factors influencing the product's chemical, morphological, and microstructural properties change. It is of great importance to optimize these production parameters in order to provide the features expected from AlSi10Mg parts. All these variables have a direct impact on the mechanical and surface properties of the parts produced [64–66]. Hence, the energy required to be given to the material in powder form for production is calculated depending on these variables as given in Eq. 1. Here, ρ_e indicates the energy that must be given per unit volume and is in the unit of J/mm^3. Laser power is expressed as L_P in Watts, e_v is the scanning speed in mm/s, h_d is the side shift amount in mm and I_t is the layer thickness in mm [67].

$$\rho_e = \frac{L_P}{e_v h_d I_t} \tag{1}$$

Here:

- L_P- Laser power (W),
- e_v-Scan speed (mm/sec),
- h_d-Hatch space (μ m),
- I_t-Layer thickness (μ m).

It is necessary to evaluate the process parameters in previous literature studies conducted with a broader perspective and correlate the results obtained from the relevant evaluations. We present the review table and the corresponding values in which the relationships of density, tensile properties, average surface roughness and hardness are presented based on experimental study (Table 1). Most of the ongoing research in this way provides an overview of experimental studies by deriving the values of many parameters based on intuition without changing the material. Therefore, based on the Taguchi experimental design, we determine the most

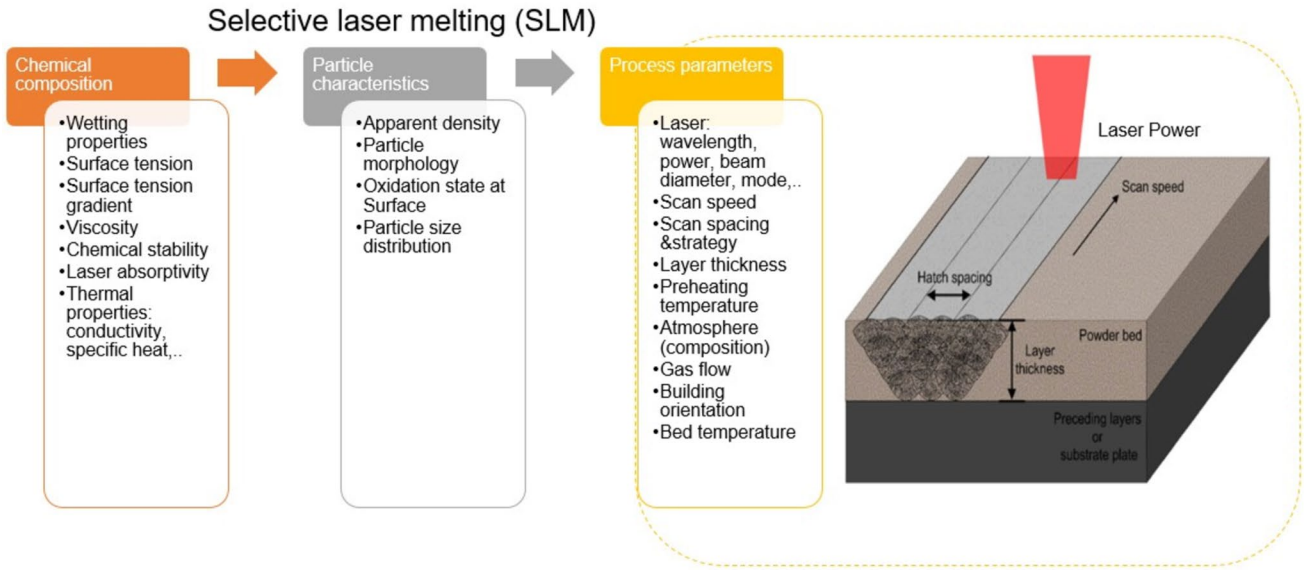

Fig. 4 Parameters affecting of SLM technologies

Table 1 Literature review of published SLM process parameters on untreated AlSi10Mg alloys

Author/ Year [Refs.]	Laser power (W)	Scan speed (mm/s)	Hatch space (μ m)	Layer thickness (μ m)	Relative Density (%)	Tensile properties, UTS (MPa)	Fatigue properties, (MPa)
Hyer et al 2020 [60]	250	1600	130	30	√ 99.1		
Hirata et al 2020 [68]	300	1200	150	30	√99.96		
Mfusi et al 2018 [69]	150	1000	50	50	√99.96		
Kempen et al. 2011 [70]	200	1200	105	30	√99.10		
Brandl et al 2012 [27]	250	500	150	50	√99.0		
Read et al 2015 [6]	175	1035	150	30	√99.0		
Aboulkhair et al. 2014 [17]	100	500	50	40	√99.77		
Yap et al 2016 [71]	350	1140	170	50	√99.8		
Raus et al 2017 [72]	350	1600	130	30	√99.13		
Zhang et al 2021 [73]	320	900	80	30	√99.86		
Gouveia et al. 2020 [74]	95	650	–	15	√98.13		
Liu et al 2019 [75]	200	-	80	25	√99.3		
Yu et al 2018 [76]	350	1150	170	50	√98.72		
Balbaa et al 2021 [77]	335	1050	150	–	√99		
Lv et al 2019 [78]	3200	12	150	50		√292	
Wei et al 2017 [10]	180	1400	–	40		√360	
Yang et al 2020 [79]	240	1600	45	–		√475.18	
Chen et al 2018 [80]	1900	8	–	–		√162	
Wang et al 2019 [81]	910	13.3	–	–		√355	
Wang et al 2018 [82]	400	–	130	–		√388	
Yan et al 2020 [83]	300	1200	140	30		√445.34	
Larrosa et al 2018 [84]	175	1025	97.5	30		√400	
Read et al 2015 [12]	175	1025	–	–		√339	
Dong et al 2019 [85]	370	1500	150	30		√360.7	
Wang et al 2019 [86]	400	500	150	30		√385	
Ch et al 2019 [87]	370	1300	190	30		√385	
Tradowsky et al. 2016 [88]	175	1025	97.5	30		√370	
Uzan et al 2018 [26]	400	1000	200	30		√358	
Girelli et al 2019 [89]	370	1300	190	30		√452	
Chen et al 2017 [90]	350	1170	240	50		√455	
Li et al 2016 [91]	350	1140	170	50		√434	
Wang et al 2018 [92]	400	1000	175	25		√358	
Buchbinder et al. 2015 [93]	960	1000	200	50		√435	
Suryawanshi et al. 2016 [94]	400	1000	175	25		√330	
Tridello et al. 2019 [95]	350	1150	170	50			√65
Zhang et al 2018 [96]	490	2000	100	40			√90
Gerov et al 2019 [97]	274	850	50	30			√100
Damon et al 2018 [98]	400	–	130	50			√77
Bagherifard et al. 2018 [99]	350	1150	170	50			√62
Lesperance et al. 2020 [100]	370	1250	100	100			√90
Ch et al 2020 [101]	370	1300	190	30			√52
Nadot et al 2020 [102]	350	930	170	50			√80
Sajada et al 2021 [103]	420	1300	210	60			√50
Wu et al 2021 [104]	400	1200	160	50			√54

Table 1 (continued)

Author/ Year [Refs.]	Laser power (W)	Scan speed (mm/s)	Hatch space (μ m)	Layer thickness (μ m)	Relative Density (%)	Tensile properties, UTS (MPa)	Fatigue properties, (MPa)
Nasab et al 2019 [105]	340	1300	200	30			√62
Aboulkhair et al. 2016 [106]	200	570	80	25			√63
Uzan et al 2017 [107]	400	1000	200	30			√62

effective design parameters by evaluating all the effects of parameters, such as laser power, scanning speed, side shift and layer thickness, together and develop a model for future studies. In this respect, an important contribution has been made to the existing literature.

2.1.1 Laser power

The employed lasers have a continuous and pulsed operation. It takes longer for continuous laser systems to reach the threshold energy required for melting or sintering than for pulsed systems because the majority of the energy transferred in continuous laser pulses is exposed to a heat flow from the beam region interacting with the laser to the material. The laser beam in pulsed laser systems acts in nanoseconds, reaching very high strengths. The heat movement from the part of the material in contact with the laser beam to the surrounding material is fairly limited because of the short contact period. As a result, it is possible to supply the threshold energy needed for melting or sintering in a lot less time [108].

The powder pool can be melted and the internal structural void concentration of the finished product can be reduced with the right side shift and scanning speed values of the fully melted structures using a powerful enough laser. More laser power is used to achieve melting, but this time, due to the melt pool's evaporation, the vapor phase does not have enough time to escape, potentially creating a keyhole effect in the melt pools [109]. As a result of this error, the density drops and the mechanical properties deteriorate. Reduced energy input from high feed speeds and insufficient laser power can be seen as an increase in surface roughness. The lower layers also do not receive enough energy flow, and the powder layer melts inside itself to produce a spherical effect from increased surface tension [110].

2.1.2 Scanning speed

The scanning speed, which indicates the speed of the laser beam on the powder layer, is represented in mm/s. While it is intended to raise the scanning speed in order to increase the production rate, the dimensional parameters of the resulting melt pool alter as the applied energy intensity lowers with higher scanning speeds. The adhesion between the layers and laser traces, which is particularly effective in mechanical characteristics, cannot be effectively given due to the dimensional deficiencies of the differentiated melt pool and the insufficient integrity between the layers and laser traces. In procedures where low scanning speeds are used, insufficient melting because insufficient laser power is supplied, increasing the number of voids, or evaporation with high laser power and low scanning speeds. Furthermore, spherication difficulty spreading powder for systems producing in the powder pool, and prevention of homogenous powder distribution may arise from the high scanning speed and high laser power utilized [111]. The linear energy density expression found in Eq. 1 has been derived by taking into account only the laser scanning speed and laser power in energy transfer. However, because the layer thickness and overlap distance are not included in this expression, the linear energy density is unable to fully express the threshold energy value required for melting. Because of the accelerating laser speed and erratic power transmission in production platforms, part quality is compromised [112].

2.1.3 Hatch space and layer thickness

For every scan track that the laser beam contacts, different linear trajectories are followed. By producing semi-melting in these various orbits, the laser guarantees the coalescence of the entire layer. All of the solid portions of the model in this layer are changed from the melt-semi-molten state to the solid state by applying a side shift amount between the generated laser traces. The distance between the centers of the melt pools of two successive laser traces is known as the hatch spacing (h_d), and it represents the lateral shifting that the laser makes. "Contour scanning" is the process of using a laser to scan the geometric boundaries when creating the geometry section [113]. You can make this shape more than once by varying the laser power or repeating the laser many times. The overlapping amounts of interior scans using contour scanning can be managed by making the planned overlapping values laterally and in the direction of laser advancement. With the power and advance value adjusted, the laser

Table 2 ANOVA for cubic model on density response

Source	Sum of Squares	df	Mean Square	F value	p value	
Model	538.05	11	48.91	25.01	< 0.0001	Significant
Power (A)	6.19	1	6.19	3.18	0.1125	
Scan speed (B)	180.08	1	180.08	92.41	< 0.0001	
Hatch space (C)	0.3259	1	0.3259	0.167	0.6933	
Layer thickness (D)	22.58	1	22.58	11.59	0.0093	
A^2	1.15	1	1.15	0.589	0.46	
B^2	11.85	1	11.85	6.08	0.0390	
C^2	0.8914	1	0.8914	0.457	0.5179	
D^2	0.5774	1	0.5774	0.296	0.6011	
A^3	0.324	1	0.324	0.166	0.6941	
B^3	76.14	1	0.3240	0.166	0.0002	
C^3	0.8035	1	0.8035	0.412	0.5387	
Residual	15.59	8	1.95			
Lack of fit	14.85	6	2.47	6.69	0.1358	Not significant
Cor Total	547.68	20				
$R^2 = 0{,}9718$			Adj $R^2 = 0.9331$			

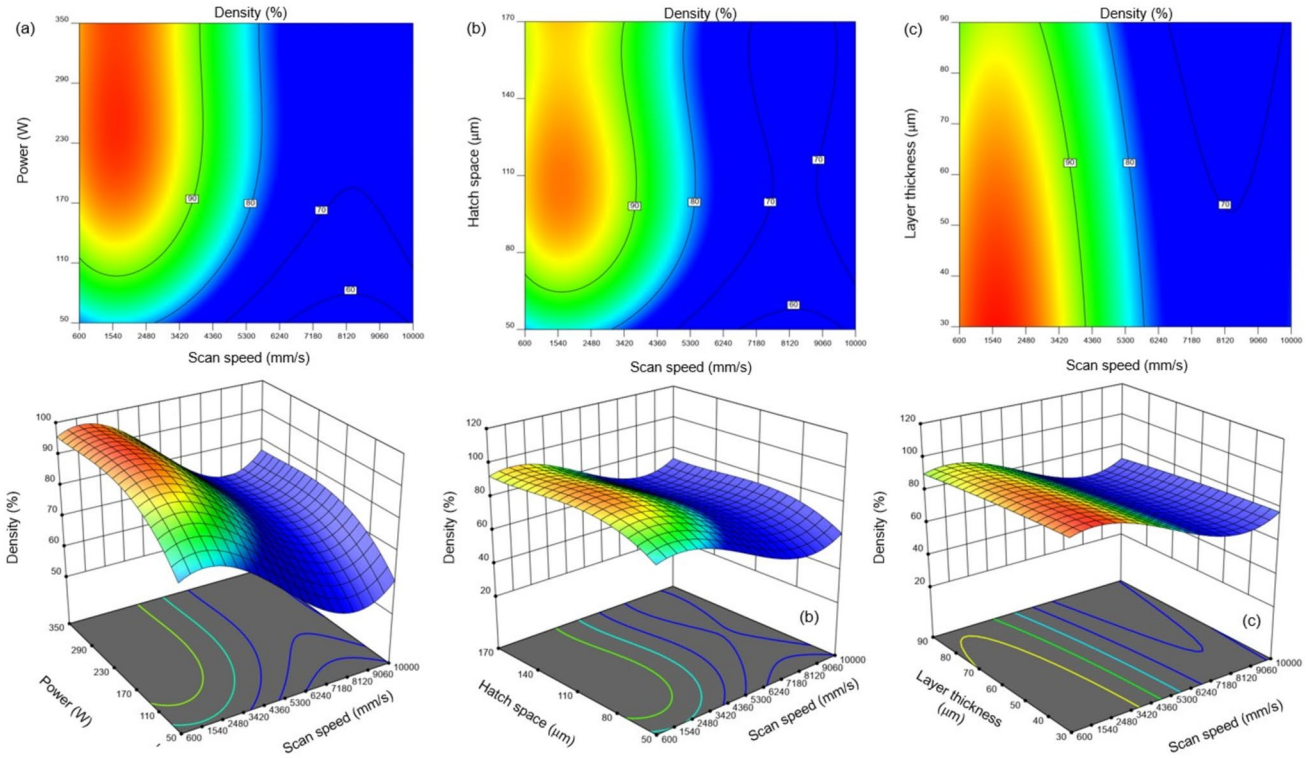

Fig. 5 Contour and 3D surface curves presenting for density power-scan speed **b** hatch space-scan speed and **c** layer thickness-scan speed

beam forms a melt pool distinct from the focal diameter when it comes in contact with the powder material [114].

The size of the melt pool that forms depends on the parameters of the scanning speed and laser power. The amount of lateral shift permits the overlap of two neighboring laser traces and, by maintaining interlayer integrity, the creation of parts with high density and strength [115]. By providing a beam offset value inward from the component boundaries, it is possible to manage the dimensional tolerance of the design and production geometries due to the melt pool that forms. Several speeds and laser power levels can be chosen for contouring and scanning tasks in SLM

Table 3 ANOVA for linear model on tensile properties response

Source	Sum of Squares	df	Mean Square	F value	*p* value	
Model	20,492,60	4	5123,15	4,11	0,0363	Significant
Power (A)	17,009,31	1	17,009,31	13,66	0,0049	
Scan speed (B)	279,63	1	279,63	0,2246	0,5865	
Hatch space (C)	46,50	1	46,50	0,0373	0,8511	
Layer thickness (D)	8530,24	1	8530,24	6,92	0,0262	
Residual	11,205,40	9	1245,04			
Lack of fit	8118,90	6	1334,41	1,30	0,4490	Not significant
Cor Total	31,698.00	13				
$R^2 = 0.99$			Adj $R^2 = 0.98$			

production. Furthermore, re-laser contact in defective locations where complete melting has not occurred can improve mechanical characteristics, reduce residual stresses, improve ballistic properties, and improve surface quality of the parts to be manufactured [116].

3 Results and discussion

In this research, we tested statistically the most effective parameters of AlSi10Mg alloys during production by selective laser melting method. ANOVA and fit statistics results were obtained for the statistical evaluation of density, tensile property and fatigue strength affected by each input parameter affecting the SLM technique presented in Table 1. Thus, both the estimated R^2 value and the adjusted R^2 values confirmed the fit statistics. However, the sources of mathematical models recommended for better performance of ANOVA results were evaluated. Therefore, the incompatibility of different combination data has been associated with the fit quality of the proposed linear, 2FI and cubic sources in order to be meaningfully derived. Design expert software program was used for this statistical evaluation. The interpretation of the input parameters in the production of AlSi10Mg alloys with SLM was determined by taking into account the P value to be less than 0.05. Additionally, Fisher's values were calculated for each process parameter. Studies in the literature on the F value in question generally state that if $F > 4$, quality results are obtained. Thus, we have presented an easy-to-understand ANOVA analysis based on contour and 3D surface curves.

3.1 Analysis of variance on density

The mathematical model of the response surface for density of laser power (A), scan speed (B), hatch space (C) and layer thickness (D) can be expressed as:

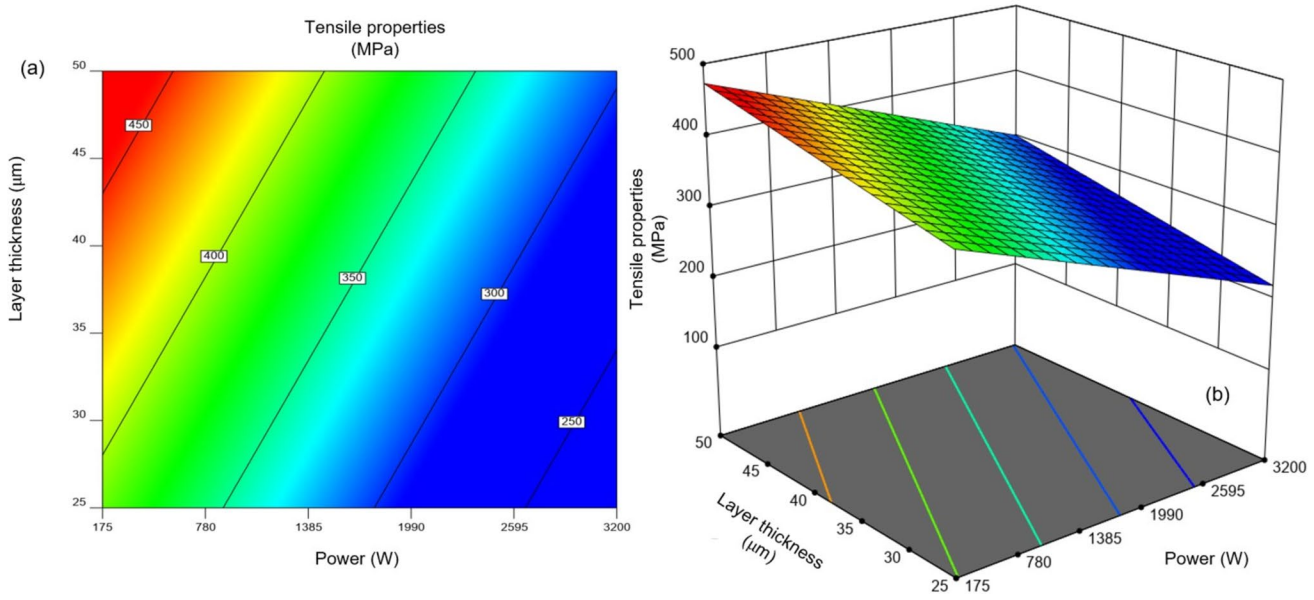

Fig. 6 Contour and 3D surface curves presenting for tensile properties **a**–**b** power-layer thickness

Table 4 ANOVA for 2FI model on fatigue properties response

Source	Sum of Squares	df	Mean Square	F value	p value	
Model	3089,44	10	308,94	126,95	0.0078	Significant
Power (A)	261,44	1	261,44	107,43	0.0092	
Scan speed (B)	128,55	1	128,55	52,82	0.0184	
Hatch space (C)	79,49	1	79,49	32,66	0.0293	
Layer thickness (D)	54,02	1	54,02	22,20	0.0422	
AB	76,78	1	76,78	31,55	0.0303	
AC	111,67	1	111,67	45,89	0.0211	
AD	16,23	1	16,23	6,67	0.1229	
BC	32,57	1	32,57	13,38	0.0673	
BD	29,48	1	29,48	12,11	0.0193	
CD	122,44	1	122,44	50,31	0.0193	
Residual	4,87	2	2,43			
Lack of fit	0,3673	1	0,3673	0,0816	0.8228	Not significant
Cor Total	3094,31	12				
$R^2 = 0.9984$			Adj $R^2 = 0.9906$			

$$\begin{aligned} Density = {} & 80{,}89 + 3{,}90A - 28{,}63B - 0{,}90C - 3{,}19D + AB + AC + AD \\ & + BC + BD + CD - 7{,}87A^2 + 4{,}05B^2 - 7{,}54C^2 - 0{,}91D^2 \\ & + ABC + ABD + ACD + BCD + A^2B + A^2D + AB^2 \\ & + AC^2 + AD^2 + B^2C + B^2D + BC^2 + BD^2 + C^2D \\ & + CD^2 + 4{,}05A^3 + 19{,}28B^3 + 6{,}69C^3 + D^3 \end{aligned} \quad (2)$$

The best performance was obtained from a cubic model to tune the parameters of the SLM technique combination of literature studies on AlSi10Mg alloy. As shown in Table 2, scanning speed and layer thickness significantly impact density. According to ANOVA, scanning speed has a very serious interaction, but there are no optimum iterations of the parameters. Therefore, scanning speed directly impacts producing samples of AlSi10Mg alloys with maximum density. Additionally, the P value in the square term of the layer thickness in the cubic model tends to be greater than 0.05, indicating non-significant terms of the model. Thus, layer thickness does not significantly affect the model's accuracy.

The contour and 3D surface images of the scanning speed in Fig. 5a, b, and c are associated with laser power, hatch space and layer thickness, respectively. The maximum response surface model prediction values of the density appear by decreasing the scan speed and increasing the laser power and hatch space, and similarly maximum values can be found at the lowest value of the layer thickness. The maximum values of the optimization functions affecting the density are indicated by the red color visual in the contour graph. The estimated optimal parameter sets correspond to values above 90% of the intensity when the scanning speed is 3420 mm/s, 230 W laser power, 110 µm hatch space and 40 µm layer thickness. This suggests that higher scanning speeds should be avoided during SLM.

3.2 Analysis of variance on tensile properties

The mathematical model of the response surface for tensile properties of laser power (A), scan speed (B), hatch space (C) and layer thickness (D) can be expressed as:

$$Tensile\ strength = 329{,}56 - 85{,}04A + 16{,}36B + 2{,}74C + 41{,}75D. \quad (3)$$

Consider Table 3, which shows the p values of the statistics of the process parameters on the tensile properties according to ANOVA. For tensile properties, the variability of the analyzed data was corrected with the linear model result of the model and its significance was tested. It can be concluded that both laser power and layer thickness have the greatest impact on the tensile properties of AlSi10Mg alloy samples produced in the SLM process. From the results for tensile properties, we can find that the p value of the laser power is 0.0049 and the layer thickness has this value with a p value of 0.0262. It shows that the scanning speed and the degree of compliance of the hatch space do not help the production of AlSi10Mg alloy by SLM within the range of the parameter data examined.

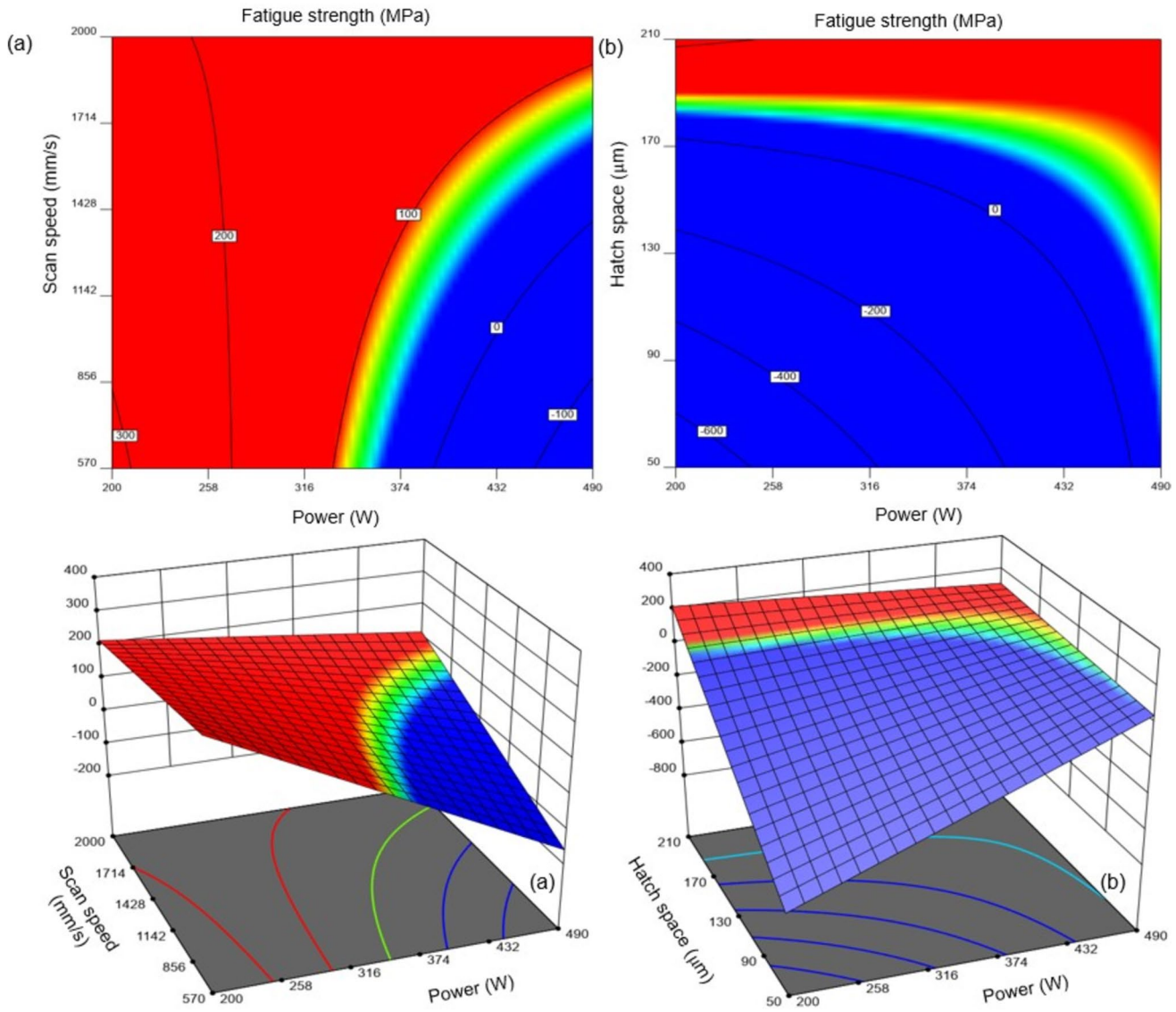

Fig. 7 Contour and 3D surface curves presenting for fatigue strength **a** scan speed-power and **b** hatch space-power

Contour graphics and 3D surface images obtained for the laser power and layer thickness affecting the tensile properties are given in Fig. 6. The mathematical model of the response surface for tensile properties of laser power, scan speed, hatch space, and layer thickness indicates that the values of tensile properties reach their maximum by decreasing laser power and increasing layer thickness. The effect of laser power on absorption properties is more evident at high layer thickness, and the effect of layer thickness is more evident at low laser power. According to ANOVA analysis, 480 W laser power and 45 µm layer thickness have the most optimum effect on tensile properties.

3.3 Analysis of variance on fatigue strength

The mathematical model of the response surface for fatigue strength of laser power (A), scan speed (B), hatch space (C) and layer thickness (D) can be expressed as:

$$\begin{aligned} \textit{Fatigue strength} = &-3{,}18 + 72{,}14A - 81{,}55B + 126{,}88C - 23{,}47D \\ &+ 94{,}49AB - 215{,}96AC - 92{,}71AD \\ &+ 124{,}78BC + 113{,}16 + 87{,}37CD \end{aligned} \quad (4)$$

ANOVA results on fatigue strength are given in detail in Table 4. The goodness of fit of the literature statistical data of AlSi10Mg alloys produced with different parameters using the SLM technique shows that the 2FI model is the most suitable.

It can be concluded that the effect of this 2FI model is laser power, scanning speed, hatch space and layer thickness. This situation was not seen in our other ANOVA analyses. Thus, it is proven that there are statistically significant interactions of parameters between the factors. This is because the examined factors had low p values. Laser power is the parameter with the highest impact on fatigue strength. Therefore, it would be much more useful to evaluate the results regarding the interactions between parameters in terms of laser power. According to ANOVA analyses, scan speed-power, and hatch space-power effects of SLM technique are effective on the fatigue strength of AlSi10Mg alloy. However, the p value of the layer thickness–power interaction is 0.1229, which shows that non-significant results cannot be drawn regarding the 2FI model.

The contour curve and 3D surface response model graph in Fig. 7 depict the relationship between scan speed–power and hatch space–power interactions and their affecting on the fatigue strength of AlSi10Mg alloys produced using the Selective Laser Melting (SLM) process. From the graph, it is observed that fatigue strength tends to increase at the lowest values of laser power and scanning speed as well as at the lowest values of laser power and highest values of hatch space. This suggests that a combination of low laser power and either low scanning speed or high hatch space can lead to higher fatigue strength in the alloy. Based on the response surface model, the optimal parameter values for achieving maximum fatigue strength were determined to be a laser power of 200 W, scanning speed of 713 mm/s, and hatch space of 210 µm. This scientific analysis indicates that specific combinations of laser power, scanning speed, and hatch space can significantly influence the fatigue strength of AlSi10Mg alloys produced by the SLM process.

4 Defense industry applications of SLM technique

4.1 Overview

SLM technology is causing a very interesting revolution in the field of defense industry. Using the SLM method, external dependency at the system, subsystem and component level can be reduced when developing products for the defense industry application field [117]. Parts produced from the inventories of tanks, armor and air defense systems, such as unmanned aerial vehicles, with which the defense industry is associated, will strengthen the ecosystem in every application and ensure its sustainability. Figure 8 shows the impact of additive manufacturing on the application area of the defense industry [118]. In this context, we have stated which questions should be answered by taking into account the scientific studies carried out and planned to be carried out on the SLM base of the defense industry. Accordingly, when we examine

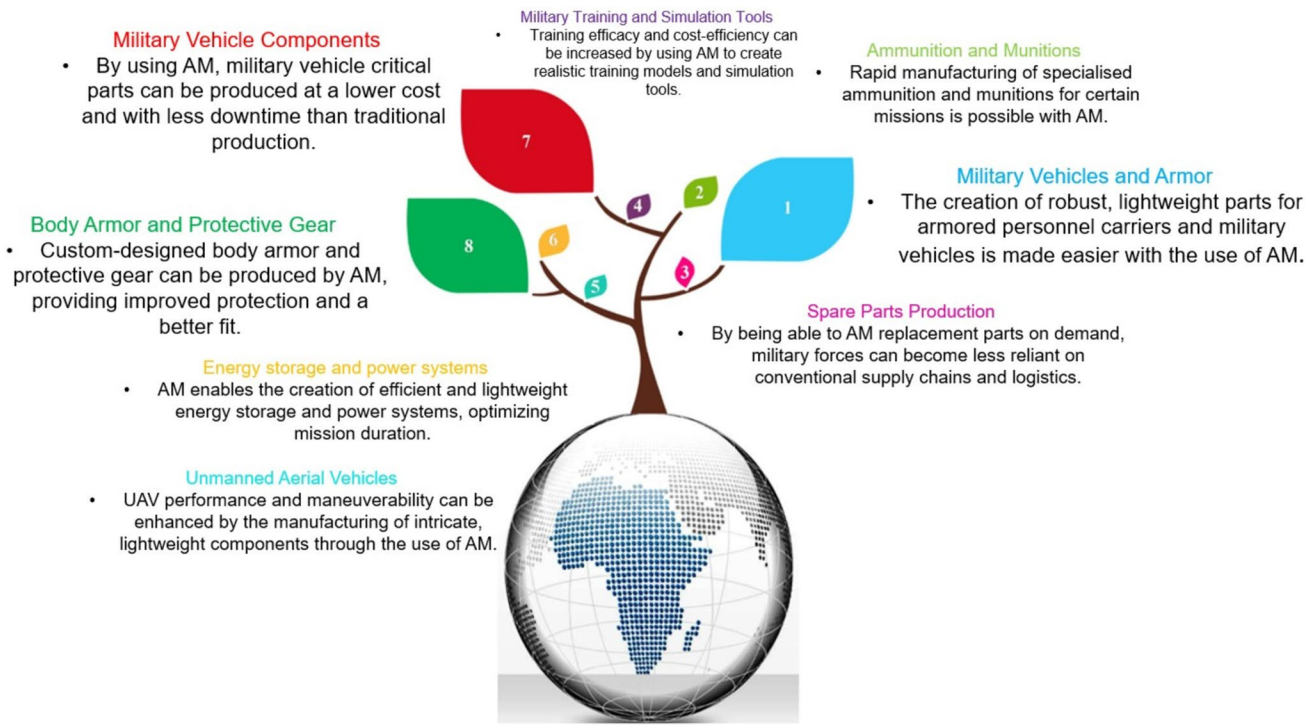

Fig. 8 New developments in defense industry

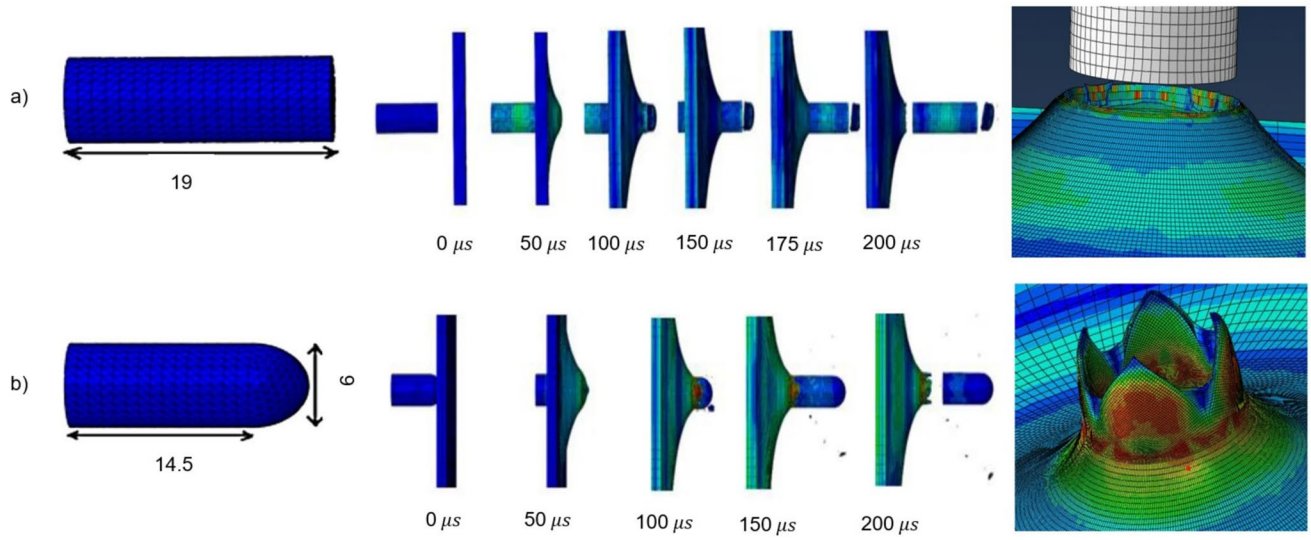

Fig. 9 Ballistic impact on 3 mm **a** blunt bullet of 225 m/s and **b** hemispherical bullet of 325 m/s [129]

the general results of 82 searches made in the last 5 years in the additive manufacturing search algorithm of armor and ballistic materials, we encounter 134 results. Different words and phrases searched in literature: ("Selective laser melting" and "armor") ("Additive manufacturing" and "ballistic") or ("Additive manufacturing" and "shock loading") or ("Selective laser melting" and "ballistic").

Reports of some studies that investigate defense industry application areas with the SLM process:

- Facchini et al. [119] studied the mechanical properties of Ti6Al4V alloy produced through SLM variants. They found martensitic microstructure, with cracks due to incomplete homologous wetting and residual stresses. Additive manufactured parts have higher tensile strength but lower ductility. Post-building heat treatment transforms metastable martensite into a biphasic a–b matrix, increasing ductility but reducing strength values. The study shows that a fully dense material can be obtained and martensite transformation can occur through SLM variations, improving ductility.
- Baufeld [120] studied Inconel 718 parts using shaped metal deposition (SLM), an additive layer manufacturing technique that produces dense, "near net-shaped" parts without pores, cracks, or fissures. The microstructure of SLM parts features large, columnar grains with a fine dendritic microstructure. Tensile tests showed no dependency on strength or strain at failure.
- Lui et al. [121] investigated the impact of microstructural factors on the ballistic velocity limit (V_{50}) of Ti6Al4V plates. The plates were created through laser powder bed fusion and direct laser metal deposition and then subjected to pre-heating or post-heating treatment. Results show that plates with martensite decomposition had higher V_{50}, while post-heating increased V_{50} due to α-lath coarsening and stress relief.
- Szachogluchowicz et al. [122] analyzed SLM M300 maraging steel behavior in ballistic testing, structural analysis, and tensile testing. Results show that annealing and aging increase ballistic properties by 87%, but increase brittleness, leading to increased perforated plate fragmentation. A detailed fracture analysis was conducted.
- Costas et al. [123] tested the ballistic performance of PBF-LB maraging steel monolithic plates and profile panels, finding the thickest heat-treated plate promising for protection. However, the material's brittleness caused fragmentation in some cases.

4.2 Material considerations

The defense industry plays a crucial role in global politics and economics, and as such, it is essential for it to continuously improve, innovate, and modernize in line with technological advancements. The global market for personal guard systems is expected to reach $15 billion by 2027, driven by rising threat levels and the need for innovative armor systems. This has led to a focus on high performance, mobility, and reduced weight armor systems [124].

The advancements in armor systems not only enhance the safety and protection of individuals but also contribute to the overall effectiveness of defense strategies. The demand for personal guard systems is being driven by the growing need for security in various sectors, including law enforcement, private security firms, and military operations. However, it is important to note that investing in armor systems may divert

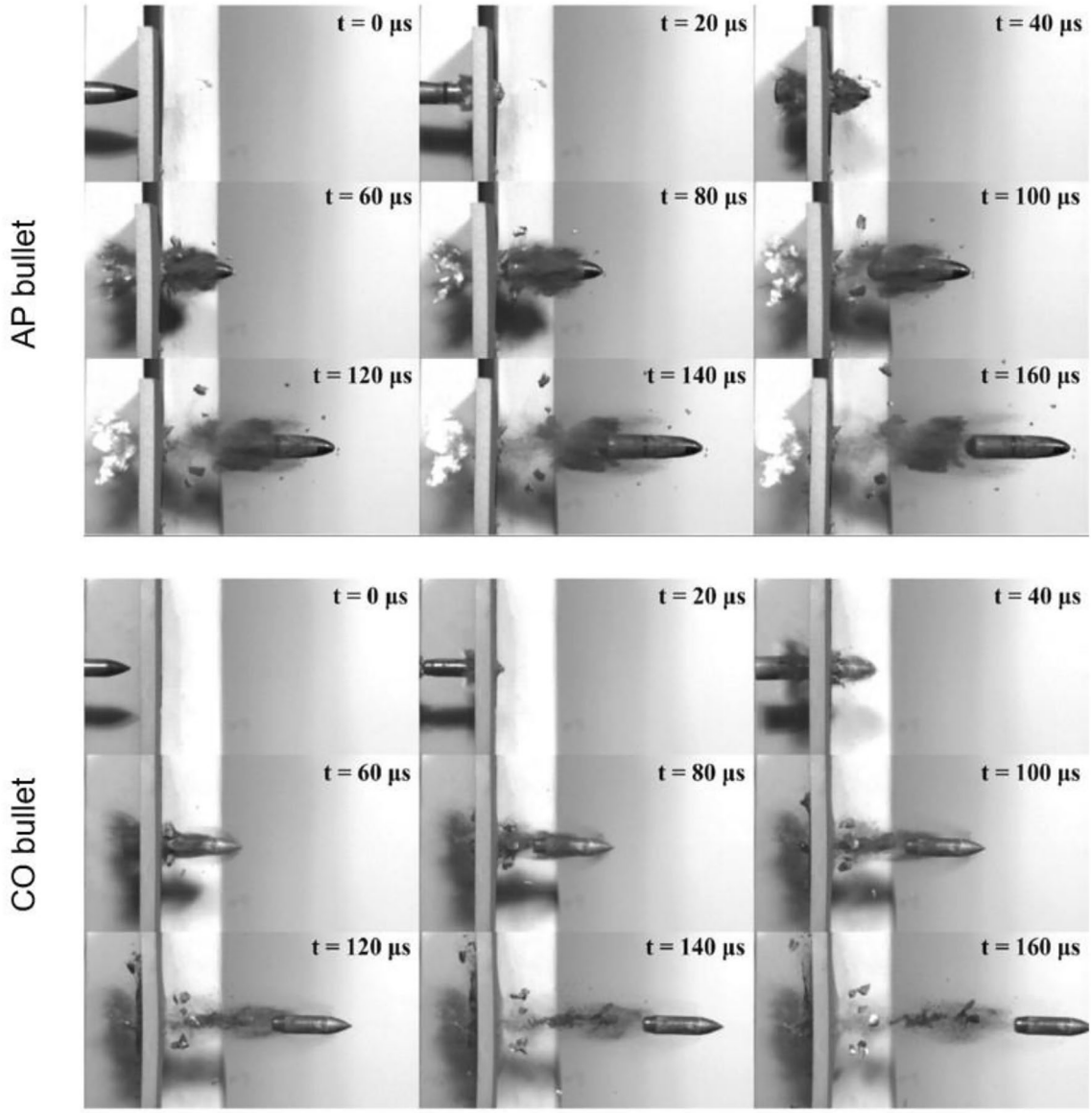

Fig. 10 The shooting images of 5 mm thick PBF-LB AlSi10Mg plates [130]

resources away from other critical defense technologies and strategies, potentially compromising overall effectiveness in the long run [125]. Additionally, the demand for personal guard systems may be limited to certain sectors and may not justify the significant investment required for their development and implementation. Therefore, while there are clear benefits to advancing armor systems, careful consideration must be given to the allocation of resources in the defense industry. Furthermore, the development of personal guard systems should also take into account the potential ethical and humanitarian implications. While enhancing security and protection is important, it is crucial to ensure that the deployment of such systems does not lead to an escalation of conflicts or human rights abuses. Moreover, the rapid pace of technological advancements in armor systems also raises concerns about the potential for misuse or unintended consequences [126].

In conclusion, while the development of novel armor systems is crucial for addressing evolving security challenges, it is important for the defense industry to carefully balance investments in these systems with other critical defense technologies and strategies [127]. Additionally, ethical considerations and potential unintended consequences should be meticulously taken into account in the development and deployment of personal guard systems. By doing this, the defense industry can effectively meet the growing demand for security while also upholding ethical and strategic considerations (Fig. 9).

4.2.1 Low velocity and ballistic performance on SLM AlSi10Mg materials

How the armor parts to be produced from AlSi10Mg alloy by SLM technique affects the optimum production parameter and low speed and ballistic impact performance is still a subject that needs to be investigated. In this regard, this compilation study was determined by taking into consideration that such a study had not been conducted when the literature in which the authors presented their opinions on the subject was systematically examined. Presently, the authors are working to address these issues.

Armor parts produced with SLM have only recently begun to be used in the field of ballistic protection, and it seems that the subject is gaining increasing importance. To this aim, Hao Xue et al. [128] stated in their studies that the use of SLM materials has a great potential in the field of ballistic penetration. They emphasized additional research into the performance of laser scanning, printing settings, and anisotropic simulation models to improve the applications of these materials in ballistics. Nirmal et al. [129] conducted a study on the impact behavior of additively manufactured AlSi10Mg alloy and the ballistic limit of projectiles using FEM simulations. Tensile tests, dynamic tests, and elevated temperature tensile tests were conducted on smooth and notched specimens. The study found that hemispherical projectiles had higher ballistic limits and impact velocity (Fig. 10).

Martin Kristoffersen et al. in a study conducted by [130], the ballistic behavior of powder bed fusion PBF-LB plates and conventional cast aluminum plates, was compared and showed that there was an almost negligible difference (the results were very close) between these two plates. In this study, AlSi10Mg metal plates with dimensions of 100 mm × 80 mm × 5 mm were produced in a PBF machine. Metallurgical studies examined the microstructure of the final alloy and determined the puncture resistance of PBF-LB plates within a ballistic range. High-speed camera images were used to measure the initial and residual velocities of different bullets. The results showed that a PBF-LB material can have similar or even better ballistic properties than conventionally produced materials with the same chemical composition. For this reason, it is expected to be an effective method on the ballistic resistance performance of AlSi10Mg parts produced by selective laser melting, which has been optimized by taking into account the cost in the compilation study.

5 Conclusions

Selective Laser Melting (SLM) technology has the potential to assist in producing inventories used in the defense industry. This paper focuses on the scientific research of AlSi10Mg alloys with SLM technology, presenting a method to optimize their mechanical properties using experimental designs of various process parameters. The study highlights the impact of changes in laser power, scanning speed, hatch space, and layer thickness on optimization results. Key findings include:

- Scanning speed directly impacts the density of AlSi10Mg alloy samples. Optimal parameter sets correspond to values above 90% intensity with a scanning speed of 3420 mm/s, 230 W laser power, 110 µm hatch space, and 40 µm layer thickness, suggesting higher scanning speeds should be avoided during SLM.
- DOE approach optimization indicates that 480 W laser power and 45 µm layer thickness have the most optimal effect on tensile properties. Maximum tensile properties are achieved by decreasing laser power and increasing layer thickness.
- A regression model for fatigue strength was developed using an RSM-based 2FI model. Optimal parameter values for maximum fatigue strength were determined to be 200 W laser power, 713 mm/s scanning speed, and 210 µm hatch space.

SLM technology offers current research and development opportunities in ballistic applications, such as low-speed impact tests. This research can help determine the interactive effects of process parameters on density, tensile properties, and fatigue strength through experimental design based on response surface methodology. No research has yet been conducted on the effects of process parameters on the ballistic behavior of AlSi10Mg alloy materials produced via this process. The authors are currently working to improve understanding and optimization of these issues to determine the appropriate manufacturing protocol.

Funding The authors would like to acknowledge funding from the Erciyes University, Turkey Scientific Research Projects Coordination Unit under research Grant No. FDK-2024–13864.

Declarations

Conflict of interest The authors declare no conflict of interest.

Ethical approval Not applicable for this work.

References

1. Girelli L, Giovagnoli M, Tocci M et al (2019) Evaluation of the impact behaviour of AlSi10Mg alloy produced using laser additive manufacturing. Mater Sci Eng A 748:38–51. https://doi.org/10.1016/j.msea.2019.01.078
2. Solyaev Y, Rabinskiy L, Tokmakov D (2019) Overmelting and closing of thin horizontal channels in AlSi10Mg samples

obtained by selective laser melting. Addit Manuf 30:100847. https://doi.org/10.1016/j.addma.2019.100847
3. Biffi CA, Fiocchi J, Tuissi A (2019) Laser Weldability of AlSi10Mg Alloy Produced by Selective Laser Melting: Microstructure and Mechanical Behavior. J Mater Eng Perform 28:6714–6719. https://doi.org/10.1007/s11665-019-04402-7
4. Nie X, Zhang H, Zhu H et al (2018) Analysis of processing parameters and characteristics of selective laser melted high strength Al-Cu-Mg alloys: From single tracks to cubic samples. J Mater Process Technol 256:69–77. https://doi.org/10.1016/j.jmatprotec.2018.01.030
5. Prashanth KG, Scudino S, Klauss HJ et al (2014) Microstructure and mechanical properties of Al-12Si produced by selective laser melting: Effect of heat treatment. Mater Sci Eng A 590:153–160. https://doi.org/10.1016/j.msea.2013.10.023
6. Ponnusamy P, Masood SH, Ruan D, et al (2020) Dynamic compressive behaviour of selective laser melted AlSi12 alloy: Effect of elevated temperature and heat treatment. Addit Manu.. https://doi.org/10.1016/j.addma.2020.101614
7. Olakanmi EO, Cochrane RF, Dalgarno KW (2015) A review on selective laser sintering/melting (SLS/SLM) of aluminium alloy powders: Processing, microstructure, and properties. Prog Mater Sci 74:401–477. https://doi.org/10.1016/j.pmatsci.2015.03.002
8. Chu F, Li E, Shen H et al (2023) Influence of powder size on defect generation in laser powder bed fusion of AlSi10Mg alloy. J Manuf Process 94:183–195. https://doi.org/10.1016/j.jmapro.2023.03.046
9. Limbasiya N, Jain A, Soni H et al (2022) A comprehensive review on the effect of process parameters and post-process treatments on microstructure and mechanical properties of selective laser melting of AlSi10Mg. J Mater Res Technol 21:1141–1176. https://doi.org/10.1016/j.jmrt.2022.09.092
10. Wei P, Wei Z, Chen Z et al (2017) The AlSi10Mg samples produced by selective laser melting: single track, densification, microstructure and mechanical behavior. Appl Surf Sci 408:38–50. https://doi.org/10.1016/j.apsusc.2017.02.215
11. Seremet H, Babacan N (2024) Compressive properties of AlSi10Mg lattice structures with novel BCCZZ and FCCZZ configurations fabricated by selective laser melting. Rapid Prototyp J 30:770–781. https://doi.org/10.1108/RPJ-06-2023-0191
12. Read N, Wang W, Essa K, Attallah MM (2015) Selective laser melting of AlSi10Mg alloy: Process optimisation and mechanical properties development. Mater Des 65:417–424. https://doi.org/10.1016/j.matdes.2014.09.044
13. Caliskan M, Hafizoglu H, Babacan N (2024) Dynamic mechanical properties of selective laser-melted AlSi10Mg lattice structures: experimental and numerical analysis with emphasis on Johnson-Cook model parameters. Int J Adv Manuf Technol 132:3861–3875. https://doi.org/10.1007/s00170-024-13570-3
14. Kanishka K, Acherjee B (2023) Revolutionizing manufacturing: A comprehensive overview of additive manufacturing processes, materials, developments, and challenges. J Manuf Process 107:574–619. https://doi.org/10.1016/j.jmapro.2023.10.024
15. Sufiiarov VS, Popovich AA, Borisov EV et al (2017) The Effect of Layer Thickness at Selective Laser Melting. Procedia Eng 174:126–134. https://doi.org/10.1016/j.proeng.2017.01.179
16. Bin AA, Pham QC (2017) Selective laser melting of AlSi10Mg: Effects of scan direction, part placement and inert gas flow velocity on tensile strength. J Mater Process Technol 240:388–396. https://doi.org/10.1016/j.jmatprotec.2016.10.015
17. Aboulkhair NT, Everitt NM, Ashcroft I, Tuck C (2014) Reducing porosity in AlSi10Mg parts processed by selective laser melting. Addit Manuf 1:77–86. https://doi.org/10.1016/j.addma.2014.08.001
18. Li Y, Gu D (2014) Parametric analysis of thermal behavior during selective laser melting additive manufacturing of aluminum alloy powder. Mater Des 63:856–867. https://doi.org/10.1016/j.matdes.2014.07.006
19. Maskery I, Aboulkhair NT, Corfield MR et al (2016) Quantification and characterisation of porosity in selectively laser melted Al-Si10-Mg using X-ray computed tomography. Mater Charact 111:193–204. https://doi.org/10.1016/j.matchar.2015.12.001
20. Boschetto A, Bottini L, Veniali F (2017) Roughness modeling of AlSi10Mg parts fabricated by selective laser melting. J Mater Process Technol 241:154–163. https://doi.org/10.1016/j.jmatprotec.2016.11.013
21. Yang T, Liu T, Liao W et al (2019) The influence of process parameters on vertical surface roughness of the AlSi10Mg parts fabricated by selective laser melting. J Mater Process Technol 266:26–36. https://doi.org/10.1016/j.jmatprotec.2018.10.015
22. Thijs L, Kempen K, Kruth JP, Van Humbeeck J (2013) Fine-structured aluminium products with controllable texture by selective laser melting of pre-alloyed AlSi10Mg powder. Acta Mater 61:1809–1819. https://doi.org/10.1016/j.actamat.2012.11.052
23. Wu J, Wang XQ, Wang W et al (2016) Microstructure and strength of selectively laser melted AlSi10Mg. Acta Mater 117:311–320. https://doi.org/10.1016/j.actamat.2016.07.012
24. Takata N, Kodaira H, Suzuki A, Kobashi M (2018) Size dependence of microstructure of AlSi10Mg alloy fabricated by selective laser melting. Mater Charact 143:18–26. https://doi.org/10.1016/j.matchar.2017.11.052
25. Rosenthal I, Stern A, Frage N (2014) Microstructure and Mechanical Properties of AlSi10Mg Parts Produced by the Laser Beam Additive Manufacturing (AM) Technology. Metallogr Microstruct Anal 3:448–453. https://doi.org/10.1007/s13632-014-0168-y
26. Uzan NE, Shneck R, Yeheskel O, Frage N (2018) High-temperature mechanical properties of AlSi10Mg specimens fabricated by additive manufacturing using selective laser melting technologies (AM-SLM). Addit Manuf 24:257–263. https://doi.org/10.1016/j.addma.2018.09.033
27. Brandl E, Heckenberger U, Holzinger V, Buchbinder D (2012) Additive manufactured AlSi10Mg samples using Selective Laser Melting (SLM): Microstructure, high cycle fatigue, and fracture behavior. Mater Des 34:159–169. https://doi.org/10.1016/j.matdes.2011.07.067
28. Maconachie T, Leary M, Zhang J et al (2020) Effect of build orientation on the quasi-static and dynamic response of SLM AlSi10Mg. Mater Sci Eng A 788:139445. https://doi.org/10.1016/j.msea.2020.139445
29. Rios JAT, Zambrano-Robledo P, Taborda JDT et al (2023) Process parameters effect and porosity reduction on AlSi10Mg parts manufactured by selective laser melting. Int J Adv Manuf Technol 129:3341–3351. https://doi.org/10.1007/s00170-023-12521-8
30. Dong Z, Xu M, Guo H et al (2022) Microstructural evolution and characterization of AlSi10Mg alloy manufactured by selective laser melting. J Mater Res Technol 17:2343–2354. https://doi.org/10.1016/j.jmrt.2022.01.129
31. Awd M, Stern F, Kampmann A, et al (2018) Microstructural characterization of the anisotropy and cyclic deformation behavior of selective laser melted AlSi10Mg structures. Metals (Basel) 8:. https://doi.org/10.3390/met8100825
32. Majeed A, Ahmed A, Salam A, Sheikh MZ (2019) Surface quality improvement by parameters analysis, optimization and heat treatment of AlSi10Mg parts manufactured by SLM additive manufacturing. Int J Light Mater Manuf 2:288–295. https://doi.org/10.1016/j.ijlmm.2019.08.001
33. Li X, Yi D, Wu X et al (2021) Effect of construction angles on microstructure and mechanical properties of AlSi10Mg

alloy fabricated by selective laser melting. J Alloys Compd 881:160459. https://doi.org/10.1016/j.jallcom.2021.160459
34. Sun J, Yang Y, Wang D (2013) Parametric optimization of selective laser melting for forming Ti6Al4V samples by Taguchi method. Opt Laser Technol 49:118–124. https://doi.org/10.1016/j.optlastec.2012.12.002
35. Wang G, Huang L, Liu Z et al (2020) Process optimization and mechanical properties of oxide dispersion strengthened nickel-based superalloy by selective laser melting. Mater Des 188:108418. https://doi.org/10.1016/j.matdes.2019.108418
36. Thango BA (2022) Application of the Analysis of Variance (ANOVA) in the Interpretation of Power Transformer Faults. Energies 15:. https://doi.org/10.3390/en15197224
37. Bibili Nzengue AG, Mpofu K, Mathe NR, Muvunzi R (2024) Optimising a processing window for the production of aluminium silicon-12 samples via selective laser melting. J Mater Res Technol 28:1062–1073. https://doi.org/10.1016/j.jmrt.2023.11.233
38. Oyesola M, Mpofu K, Mathe N et al (2021) Optimization of selective laser melting process parameters for surface quality performance of the fabricated Ti6Al4V. Int J Adv Manuf Technol 114:1585–1599. https://doi.org/10.1007/s00170-021-06953-3
39. Liu Y, Liu C, Liu W et al (2019) Optimization of parameters in laser powder deposition AlSi10Mg alloy using Taguchi method. Opt Laser Technol 111:470–480. https://doi.org/10.1016/j.optlastec.2018.10.030
40. Schleifenbaum H, Meiners W, Wissenbach K, Hinke C (2010) Individualized production by means of high power Selective Laser Melting. CIRP J Manuf Sci Technol 2:161–169. https://doi.org/10.1016/j.cirpj.2010.03.005
41. Zhang J, Song B, Wei Q et al (2019) A review of selective laser melting of aluminum alloys: Processing, microstructure, property and developing trends. J Mater Sci Technol 35:270–284. https://doi.org/10.1016/j.jmst.2018.09.004
42. DebRoy T, Wei HL, Zuback JS et al (2018) Additive manufacturing of metallic components – Process, structure and properties. Prog Mater Sci 92:112–224. https://doi.org/10.1016/j.pmatsci.2017.10.001
43. Mousa AA, Bashir MO (2017) Additive Manufacturing: A New Industrial Revolution-A Review. J Sci Achiev 2:19–31
44. Herzog D, Seyda V, Wycisk E, Emmelmann C (2016) Additive manufacturing of metals. Acta Mater 117:371–392. https://doi.org/10.1016/j.actamat.2016.07.019
45. Ngo TD, Kashani A, Imbalzano G et al (2018) Additive manufacturing (3D printing): A review of materials, methods, applications and challenges. Compos Part B Eng 143:172–196. https://doi.org/10.1016/j.compositesb.2018.02.012
46. Karunakaran KP, Bernard A, Suryakumar S et al (2012) Rapid manufacturing of metallic objects. Rapid Prototyp J 18:264–280. https://doi.org/10.1108/13552541211231644
47. Seabra M, Azevedo J, Araújo A et al (2016) Selective laser melting (SLM) and topology optimization for lighter aerospace componentes. Procedia Struct Integr 1:289–296. https://doi.org/10.1016/j.prostr.2016.02.039
48. Eyers DR, Potter AT (2017) Industrial Additive Manufacturing: A manufacturing systems perspective. Comput Ind 92–93:208–218. https://doi.org/10.1016/j.compind.2017.08.002
49. Gao W, Zhang Y, Ramanujan D et al (2015) The status, challenges, and future of additive manufacturing in engineering. CAD Comput Aided Des 69:65–89. https://doi.org/10.1016/j.cad.2015.04.001
50. Ford S, Despeisse M, Viljakainen A (2015) Extending product life through additive manufacturing : The sustainability implications. Glob Clean Prod Consum Conf 1–4
51. Rouf S, Malik A, Singh N et al (2022) Additive manufacturing technologies: Industrial and medical applications. Sustain Oper Comput 3:258–274. https://doi.org/10.1016/j.susoc.2022.05.001
52. Kumar R, Kumar M, Chohan JS (2021) The role of additive manufacturing for biomedical applications: A critical review. J Manuf Process 64:828–850. https://doi.org/10.1016/j.jmapro.2021.02.022
53. Bak D (2003) Rapid prototyping or rapid production? 3D printing processes move industry towards the latter. Assem Autom 23:340–345. https://doi.org/10.1108/01445150310501190
54. Attaran M (2017) The rise of 3-D printing: The advantages of additive manufacturing over traditional manufacturing. Bus Horiz 60:677–688. https://doi.org/10.1016/j.bushor.2017.05.011
55. Kruth JP, Mercelis P, Van Vaerenbergh J et al (2005) Binding mechanisms in selective laser sintering and selective laser melting. Rapid Prototyp J 11:26–36. https://doi.org/10.1108/13552540510573365
56. Nandhakumar R, Venkatesan K (2023) A process parameters review on selective laser melting-based additive manufacturing of single and multi-material: Microstructure, physical properties, tribological, and surface roughness. Elsevier Ltd
57. Thijs L, Verhaeghe F, Craeghs T et al (2010) A study of the microstructural evolution during selective laser melting of Ti-6Al-4V. Acta Mater 58:3303–3312. https://doi.org/10.1016/j.actamat.2010.02.004
58. Kruth JP, Levy G, Klocke F, Childs THC (2007) Consolidation phenomena in laser and powder-bed based layered manufacturing. CIRP Ann - Manuf Technol 56:730–759. https://doi.org/10.1016/j.cirp.2007.10.004
59. Lupi F, Pacini A, Lanzetta M (2023) Laser powder bed additive manufacturing: A review on the four drivers for an online control. J Manuf Process 103:413–429. https://doi.org/10.1016/j.jmapro.2023.08.022
60. Hyer H, Zhou L, Park S et al (2020) Understanding the Laser Powder Bed Fusion of AlSi10Mg Alloy. Metallogr Microstruct Anal 9:484–502. https://doi.org/10.1007/s13632-020-00659-w
61. Yadroitsev I, Bertrand P, Smurov I (2007) Parametric analysis of the selective laser melting process. Appl Surf Sci 253:8064–8069. https://doi.org/10.1016/j.apsusc.2007.02.088
62. Gu DD, Meiners W, Wissenbach K, Poprawe R (2012) Laser additive manufacturing of metallic components: Materials, processes and mechanisms. Int Mater Rev 57:133–164. https://doi.org/10.1179/1743280411Y.0000000014
63. Yusuf SM, Gao N (2017) Influence of energy density on metallurgy and properties in metal additive manufacturing. Mater Sci Technol (United Kingdom) 33:1269–1289. https://doi.org/10.1080/02670836.2017.1289444
64. Krishnan M, Atzeni E, Canali R et al (2014) On the effect of process parameters on properties of AlSi10Mg parts produced by DMLS. Rapid Prototyp J 20:449–458. https://doi.org/10.1108/RPJ-03-2013-0028
65. Gençoğlu U, Kaya G, Ergüder TO et al (2022) Investigation of the structural and tribological properties of 316L stainless steel manufactured using variable production parameters by selective laser melting. J Mater Eng Perform 31:3688–3703. https://doi.org/10.1007/s11665-021-06507-4
66. Xue G, Ke L, Zhu H, et al (2019) Influence of processing parameters on selective laser melted SiCp/AlSi10Mg composites: Densification, microstructure and mechanical properties. Mater Sci Eng A 764:. https://doi.org/10.1016/j.msea.2019.138155
67. Singla AK, Banerjee M, Sharma A et al (2021) Selective laser melting of Ti6Al4V alloy: Process parameters, defects and post-treatments. J Manuf Process 64:161–187. https://doi.org/10.1016/j.jmapro.2021.01.009
68. Hirata T, Kimura T, Nakamoto T (2020) Effects of hot isostatic pressing and internal porosity on the performance of selective

laser melted AlSi10Mg alloys. Mater Sci Eng A 772:138713. https://doi.org/10.1016/j.msea.2019.138713
69. Mfusi BJ, Tshabalala LC, Popoola API, Mathe NR (2018) The effect of selective laser melting build orientation on the mechanical properties of AlSi10Mg parts. IOP Conf Ser Mater Sci Eng 430:. https://doi.org/10.1088/1757-899X/430/1/012028
70. Kempen K, Thijs L, Yasa E, et al (2011) Process optimization and microstructural analysis for selective laser melting of AlSi10Mg. 22nd Annu Int Solid Free Fabr Symp - An Addit Manuf Conf SFF 2011 484–495
71. Yap CY, Chua CK, Dong ZL (2016) An effective analytical model of selective laser melting. Virtual Phys Prototyp 11:21–26. https://doi.org/10.1080/17452759.2015.1133217
72. A.A R, M.S W, M. I, et al (2016) Mechanical and Physical Properties of AlSi10Mg Processed through Selective Laser Melting. Int J Eng Technol 8:2612–2618. https://doi.org/10.21817/ijet/2016/v8i6/160806217
73. Zhang Y, Majeed A, Muzamil M et al (2021) Investigation for macro mechanical behavior explicitly for thin-walled parts of AlSi10Mg alloy using selective laser melting technique. J Manuf Process 66:269–280. https://doi.org/10.1016/j.jmapro.2021.04.022
74. Parts A, Alves JL materials E ff ect of Scan Strategies and Use of Support Structures on Surface Quality and Hardness of L-PBF
75. Liu B, Li BQ, Li Z (2019) Selective laser remelting of an additive layer manufacturing process on AlSi10Mg. Results Phys 12:982–988. https://doi.org/10.1016/j.rinp.2018.12.018
76. Yu WH, Sing SL, Tian XL, Chua CK (2018) Effects of re-melting strategies on densification behavior and mechanical properties of selective laser melting ALSI10MG parts. Proc Int Conf Prog Addit Manuf 2018-May:476–481. https://doi.org/10.25341/D48309
77. Balbaa MA, Ghasemi A, Fereiduni E et al (2021) Role of powder particle size on laser powder bed fusion processability of AlSi10mg alloy. Addit Manuf 37:101630. https://doi.org/10.1016/j.addma.2020.101630
78. Lv F, Shen L, Liang H et al (2019) Mechanical properties of AlSi10Mg alloy fabricated by laser melting deposition and improvements via heat treatment. Optik (Stuttg) 179:8–18. https://doi.org/10.1016/j.ijleo.2018.10.112
79. Yang T, Liu T, Liao W et al (2020) Laser powder bed fusion of AlSi10Mg: Influence of energy intensities on spatter and porosity evolution, microstructure and mechanical properties. J Alloys Compd 849:156300. https://doi.org/10.1016/j.jallcom.2020.156300
80. Chen B, Yao Y, Song X et al (2018) Microstructure and mechanical properties of additive manufacturing AlSi10Mg alloy using direct metal deposition. Ferroelectrics 523:153–166. https://doi.org/10.1080/00150193.2018.1392147
81. Wang X, Li L, Qu J, Tao W (2019) Microstructure and mechanical properties of laser metal deposited AlSi10Mg alloys. Mater Sci Technol (United Kingdom) 35:2284–2293. https://doi.org/10.1080/02670836.2019.1674022
82. Wang L, zhi, Wang S, Hong X, (2018) Pulsed SLM-manufactured AlSi10Mg alloy: Mechanical properties and microstructural effects of designed laser energy densities. J Manuf Process 35:492–499. https://doi.org/10.1016/j.jmapro.2018.09.007
83. Yan Q, Song B, Shi Y (2020) Comparative study of performance comparison of AlSi10Mg alloy prepared by selective laser melting and casting. J Mater Sci Technol 41:199–208. https://doi.org/10.1016/j.jmst.2019.08.049
84. Larrosa NO, Wang W, Read N et al (2018) Linking microstructure and processing defects to mechanical properties of selectively laser melted AlSi10Mg alloy. Theor Appl Fract Mech 98:123–133. https://doi.org/10.1016/j.tafmec.2018.09.011
85. Dong Z, Liu Y, Li W, Liang J (2019) Orientation dependency for microstructure, geometric accuracy and mechanical properties of selective laser melting AlSi10Mg lattices. J Alloys Compd 791:490–500. https://doi.org/10.1016/j.jallcom.2019.03.344
86. Wang L, Jiang X, Zhu Y, et al (2018) Investigation of Performance and Residual Stress Generation of AlSi10Mg Processed by Selective Laser Melting. Adv Mater Sci Eng 2018. https://doi.org/10.1155/2018/7814039
87. Ch SR, Raja A, Nadig P et al (2019) Influence of working environment and built orientation on the tensile properties of selective laser melted AlSi10Mg alloy. Mater Sci Eng A 750:141–151. https://doi.org/10.1016/j.msea.2019.01.103
88. Tradowsky U, White J, Ward RM et al (2016) Selective laser melting of AlSi10Mg: Influence of post-processing on the microstructural and tensile properties development. Mater Des 105:212–222. https://doi.org/10.1016/j.matdes.2016.05.066
89. Girelli L, Tocci M, Gelfi M, Pola A (2019) Study of heat treatment parameters for additively manufactured AlSi10Mg in comparison with corresponding cast alloy. Mater Sci Eng A 739:317–328. https://doi.org/10.1016/j.msea.2018.10.026
90. Chen B, Moon SK, Yao X et al (2017) Strength and strain hardening of a selective laser melted AlSi10Mg alloy. Scr Mater 141:45–49. https://doi.org/10.1016/j.scriptamat.2017.07.025
91. Li W, Li S, Liu J et al (2016) Effect of heat treatment on AlSi10Mg alloy fabricated by selective laser melting: Microstructure evolution, mechanical properties and fracture mechanism. Mater Sci Eng A 663:116–125. https://doi.org/10.1016/j.msea.2016.03.088
92. Wang LF, Sun J, Yu XL et al (2018) Enhancement in mechanical properties of selectively laser-melted AlSi10Mg aluminum alloys by T6-like heat treatment. Mater Sci Eng A 734:299–310. https://doi.org/10.1016/j.msea.2018.07.103
93. Buchbinder D, Meiners W, Wissenbach K, Poprawe R (2015) Selective laser melting of aluminum die-cast alloy—Correlations between process parameters, solidification conditions, and resulting mechanical properties. J Laser Appl. https://doi.org/10.2351/1.4906389
94. Suryawanshi J, Prashanth KG, Scudino S et al (2016) Simultaneous enhancements of strength and toughness in an Al-12Si alloy synthesized using selective laser melting. Acta Mater 115:285–294. https://doi.org/10.1016/j.actamat.2016.06.009
95. Tridello A, Fiocchi J, Biffi CA et al (2019) VHCF response of Gaussian SLM AlSi10Mg specimens: Effect of a stress relief heat treatment. Int J Fatigue 124:435–443. https://doi.org/10.1016/j.ijfatigue.2019.02.020
96. Zhang C, Zhu H, Liao H et al (2018) Effect of heat treatments on fatigue property of selective laser melting AlSi10Mg. Int J Fatigue 116:513–522. https://doi.org/10.1016/j.ijfatigue.2018.07.016
97. Gerov MV, Vladislavskaya EY, Terent'ev VF, et al (2019) Fatigue Strength of an AlSi10Mg Alloy Fabricated by Selective Laser Melting. Russ Metall 2019:392–397. https://doi.org/10.1134/S0036029519040098
98. Damon J, Dietrich S, Vollert F et al (2018) Process dependent porosity and the influence of shot peening on porosity morphology regarding selective laser melted AlSi10Mg parts. Addit Manuf 20:77–89. https://doi.org/10.1016/j.addma.2018.01.001
99. Bagherifard S, Beretta N, Monti S et al (2018) On the fatigue strength enhancement of additive manufactured AlSi10Mg parts by mechanical and thermal post-processing. Mater Des 145:28–41. https://doi.org/10.1016/j.matdes.2018.02.055
100. Lesperance X, Ilie P, Ince A (2021) Very high cycle fatigue characterization of additively manufactured AlSi10Mg and AlSi7Mg aluminium alloys based on ultrasonic fatigue testing. Fatigue Fract Eng Mater Struct 44:876–884. https://doi.org/10.1111/ffe.13406

101. Ch SR, Raja A, Jayaganthan R et al (2020) Study on the fatigue behaviour of selective laser melted AlSi10Mg alloy. Mater Sci Eng A 781:139180. https://doi.org/10.1016/j.msea.2020.139180
102. Nadot Y, Nadot-Martin C, Kan WH et al (2020) Predicting the fatigue life of an AlSi10Mg alloy manufactured via laser powder bed fusion by using data from computed tomography. Addit Manuf 32:100899. https://doi.org/10.1016/j.addma.2019.100899
103. Sajadi F, Tiemann JM, Bandari N et al (2021) Fatigue improvement of alsi10mg fabricated by laser-based powder bed fusion through heat treatment. Metals (Basel) 11:1–17. https://doi.org/10.3390/met11050683
104. Wu Z, Wu S, Bao J et al (2021) The effect of defect population on the anisotropic fatigue resistance of AlSi10Mg alloy fabricated by laser powder bed fusion. Int J Fatigue 151:106317. https://doi.org/10.1016/j.ijfatigue.2021.106317
105. Nasab MH, Giussani A, Gastaldi D et al (2019) Effect of surface and subsurface defects on fatigue behavior of AlSi10Mg alloy processed by laser powder bed fusion (L-PBF). Metals (Basel) 9:7–10. https://doi.org/10.3390/met9101063
106. Aboulkhair NT, Maskery I, Tuck C et al (2016) Improving the fatigue behaviour of a selectively laser melted aluminium alloy: Influence of heat treatment and surface quality. Mater Des 104:174–182. https://doi.org/10.1016/j.matdes.2016.05.041
107. Uzan NE, Shneck R, Yeheskel O, Frage N (2017) Fatigue of AlSi10Mg specimens fabricated by additive manufacturing selective laser melting (AM-SLM). Mater Sci Eng A 704:229–237. https://doi.org/10.1016/j.msea.2017.08.027
108. Buchbinder D, Schleifenbaum H, Heidrich S et al (2011) High power Selective Laser Melting (HP SLM) of aluminum parts. Phys Procedia 12:271–278. https://doi.org/10.1016/j.phpro.2011.03.035
109. Pinkerton AJ (2016) [INVITED] Lasers in additive manufacturing. Opt Laser Technol 78:25–32. https://doi.org/10.1016/j.optlastec.2015.09.025
110. Lee H, Lim CHJ, Low MJ et al (2017) Lasers in additive manufacturing: A review. Int J Precis Eng Manuf - Green Technol 4:307–322. https://doi.org/10.1007/s40684-017-0037-7
111. Yoo HW, Ito S, Schitter G (2016) High speed laser scanning microscopy by iterative learning control of a galvanometer scanner. Control Eng Pract 50:12–21. https://doi.org/10.1016/j.conengprac.2016.02.007
112. Dilip JJS, Anam MA, Pal D, Stucker B (2016) A short study on the fabrication of single track deposits in SLM and characterization. Solid Free Fabr 2016 Proc 27th Annu Int Solid Free Fabr Symp - An Addit Manuf Conf SFF 2016 1644–1659
113. Scipioni Bertoli U, Wolfer AJ, Matthews MJ et al (2017) On the limitations of volumetric energy density as a design parameter for selective laser melting. Mater Des 113:331–340. https://doi.org/10.1016/j.matdes.2016.10.037
114. Rombouts M (2006) Selective Laser Sintering/Melting of Iron-Based Powders. 268
115. Ghouse S, Babu S, Van Arkel RJ et al (2017) The influence of laser parameters and scanning strategies on the mechanical properties of a stochastic porous material. Mater Des 131:498–508. https://doi.org/10.1016/j.matdes.2017.06.041
116. Roberto A, Bineli R (2011) Direct Metal Laser Sintering (Dmls): Technology for Design and Construction of Microreactors
117. Markovsky PE, Ivasishin OM, Savvakin DG, et al (2022) Titanium-Based Layered Armour Elements Manufacture with 3D-Printing Approach. Metallofiz i Noveishie Tekhnologii . https://doi.org/10.15407/mfint.44.10.1361
118. Colorado HA, Cardenas CA, Gutierrez-Velazquez EI et al (2023) Additive manufacturing in armor and military applications: research, materials, processing technologies, perspectives, and challenges. J Mater Res Technol 27:3900–3913. https://doi.org/10.1016/j.jmrt.2023.11.030
119. Facchini L, Magalini E, Robotti P et al (2010) Ductility of a Ti-6Al-4V alloy produced by selective laser melting of prealloyed powders. Rapid Prototyp J 16:450–459. https://doi.org/10.1108/13552541011083371
120. Baufeld B (2012) Mechanical properties of INCONEL 718 parts manufactured by shaped metal deposition (SMD). J Mater Eng Perform 21:1416–1421. https://doi.org/10.1007/s11665-011-0009-y
121. Lui EW, Medvedev AE, Edwards D et al (2022) Microstructure modification of additive manufactured Ti-6Al-4V plates for improved ballistic performance properties. J Mater Process Technol 301:117436. https://doi.org/10.1016/j.jmatprotec.2021.117436
122. Fikus B, Grzelak K, Torzewski J (2021) Selective laser melted M300 maraging steel—material. Materials (Basel). https://doi.org/10.3390/ma14102681
123. Costas M, Edwards-Mowforth M, Kristoffersen M et al (2021) Ballistic impact resistance of additive manufactured high-strength maraging steel: An experimental study. Int J Prot Struct 12:577–603. https://doi.org/10.1177/20414196211035486
124. Rahmani R, Antonov M, Brojan M (2020) Lightweight 3D printed Ti6Al4V-AlSi10Mg hybrid composite for impact resistance and armor piercing shielding. J Mater Res Technol 9:13842–13854. https://doi.org/10.1016/j.jmrt.2020.09.108
125. Coltelli MA, Catterlin J, Scherer A, Kartalov EP (2021) Simulations of 3D-Printable biomimetic artificial muscles based on microfluidic microcapacitors for exoskeletal actuation and stealthy underwater propulsion. Sensors Actuators, A Phys 325:112700. https://doi.org/10.1016/j.sna.2021.112700
126. Bonnín Roca J, Vaishnav P, Morgan MG et al (2017) When risks cannot be seen: Regulating uncertainty in emerging technologies. Res Policy 46:1215–1233. https://doi.org/10.1016/j.respol.2017.05.010
127. Bhat A, Naveen J, Jawaid M et al (2021) Advancement in fiber reinforced polymer, metal alloys and multi-layered armour systems for ballistic applications – A review. J Mater Res Technol 15:1300–1317. https://doi.org/10.1016/j.jmrt.2021.08.150
128. Xue H, Wang T, Cui X, yu, et al (2023) On the ballistic perforation performance of additively manufactured 316 L stainless steel cylindrical projectiles. Int J Impact Eng. https://doi.org/10.1016/j.ijimpeng.2023.104625
129. Nirmal RR, Patnaik BSV, Jayaganthan R (2021) FEM simulation of high speed impact behaviour of additively manufactured AlSi10Mg alloy. J Dyn Behav Mater 7:469–484. https://doi.org/10.1007/s40870-020-00285-1
130. Kristoffersen M, Costas M, Koenis T et al (2020) On the ballistic perforation resistance of additive manufactured AlSi10Mg aluminium plates. Int J Impact Eng. https://doi.org/10.1016/j.ijimpeng.2019.103476